Microstructure of the heliospheric termination shock: Full particle electrodynamic simulations

Matsukiyo, Shuichi
Department of Earth System Science and Technology, Kyushu University | Kyushu University : Assistant Professor

Scholer, Manfred
Max-Planck-Institut für Extraterrestrische Physik | Kyushu University : Assistant Professor

出版情報：Journal of Geophysical Research. 116 (A8), pp.A08106-1-A08106-12, 2011-08-26. American Geophysical Union
バージョン：
権利関係：

Microstructure of the heliospheric termination shock: Full particle electrodynamic simulations

Shuichi Matsukiyo[1] and Manfred Scholer[1,2]

Shuichi Matsukiyo, Department of Earth System Science and Technology, Kyushu University, 6-1 Kasuga-Koen, Kasuga 816-8580 Fukuoka, Japan.

Manfred Scholer, Max-Planck-Institut f. extraterrestrische Physik, P.O. Box 1604, 85740 Garching, Germany.

[1]Department of Earth System Science and Technology, Kyushu University, Fukuoka, Japan.

[2]Max-Planck-Institut f. extraterrestrische Physik, Garching, Germany.

Abstract. A particle-in-cell (PIC) code is used to examine kinetic properties of pickup ions at the heliospheric termination shock. The code treats the pickup ions self-consistently as a third component. The simulations are one-dimensional in spatial variations. We use a relative pickup ion density of 30% and two different values of the magnetic field - shock normal angle, $\Theta_{Bn} = 90°$ and $\Theta_{Bn} = 87°$, respectively. The oblique shock is chosen in order to allow for wave vectors parallel to the magnetic field due to instabilities in the foot. In addition a run is presented with a 60% relative pickup ion density to investigate a pickup ion dominated shock. Upstream of the ramp is an extended foot due to reflected pickup ions. In this foot the magnetic field continuously increases and the bulk speed of the pickup ions as well as the bulk speed of the solar wind ions decrease and reach at the magnetic field ramp the downstream value. The positive bulk velocity of the pickup ions in the extended foot perpendicular to the magnetic field and to the shock normal causes an electric field in the shock normal direction. This leads to a large increase of the shock potential well upstream of the magnetic field ramp. The maximum value of the potential is $\sim$ 0.35 the shock ram energy and is by a factor 5 larger than expected for a weak shock without pickup ions. Pickup ion reflection at the shock is almost 100%; part of the pickup ions are essentially specularly reflected by the magnetic field force term of the Lorentz force in the overshoot, part are reflected in the extended foot due to a combination of magnetic force term and the cross-shock potential. In the 30% pickup ion case about 90% of the total thermal energy gain in

the shock is gained by pickup ions, a little under 10% by the solar wind ions. The thermal energy gain by pickup ions increases as the pickup ion relative density increases. The pickup ion temperature increases continuously from the upstream edge of the extended foot to the shock ramp and stays then constant through the overshoot and downstream.

1. Introduction

Direct observations by Voyager 1 (V1) and 2 (V2) and indirect observations by IBEX have dramatically increased in recent years our knowledge of the heliospheric termination shock and the region beyond. V1 crossed the termination shock in December 2004 at a distance of 94 AU [*Stone et al.* , 2005] and V2 crossed the termination shock in August 2007 at 84 AU [*Decker et al.* , 2008]. Both Voyager spacecraft provided magnetic field data during the crossings [*Burlaga et al.* , 2005], [*Burlaga et al.* , 2008], however only V2 provided plasma measurements in the thermal energy range. From the plasma measurements it was concluded that solar wind ions account for only 15% of the dissipation at the termination shock [*Richardson et al.* , 2008]. *Richardson* [2008] suggested that pickup ions, not seen by the plasma instrument, account for most of the dissipation. Pickup ions are the interstellar neutral atoms which are ionized in the heliosphere and picked up by the solar wind. The Earth-orbiting IBEX spacecraft, launched in October 2008, measures the energetic neutral atoms (ENAs) which are produced by charge-exchange between the heated solar wind in the heliosheath and cold neutral from the interstellar medium [*McComas et al.* , 2009]. The flux of ENAs depends on the high energy tail of the distribution function of the combined heated solar wind ions and pickup ions downstream of the termination shock. Interpretation of observations by Voyager and IBEX thus depends on the process of solar wind and pickup ion heating through the termination shock.

A number of analytical models and computational simulations have been concerned in the past with the partition of dissipation energy between solar wind ions and pickup ions and with the acceleration mechanism/mechanisms of pickup ions to higher energies.

Lee et al. [1996] and *Zank et al.* [1996] have investigated the possibility that pickup ions are accelerated at quasi-perpendicular shock by so-called shock surfing, where part of the pickup ions incident on the shock are trapped between the electrostatic potential of the shock and the upstream Lorentz force. The efficiency of this mechanism strongly depends on the scale of the cross-shock potential: the surfing mechanism, also called multiply reflected ion (MRI) mechanism, is only efficient when the scale of the cross-shock potential is of the order of the electron inertial length. *Zank et al.* [1996] have proposed that the MRI mechanism works as a pickup ion injection mechanism into a first order Fermi acceleration mechanism at the termination shock.

Early computational simulations of collisionless shocks in a solar wind containing a large percentage of pickup ions used the hybrid method where ions are treated as (macro-)particles and the electrons are treated as either a massless or finite-mass fluid. *Liewer et al.* [1993] showed by hybrid simulations of a shock with an upstream relative pickup ion density of 20% that an extended foot exists upstream of the ramp of the size of the pickup ion gyroradius. In their simulation the solar wind ions provided most of the shock dissipation. *Kucharek and Scholer* [1995] also performed hybrid simulations of pickup loaded shocks. However, these authors were mostly concerned with the possibility of injecting pickup ions into a diffusive acceleration process and argued that when Θ_{Bn}, the angle between the upstream magnetic field and the shock normal, is less than 70° pickup ions can escape upstream and can take part in a diffusive acceleration process. Hybrid simulations with a finite electron mass fluid were reported by *Lipatov and Zank* [1999]. These authors found that pickup ions gained high energies through multiple reflections by the cross-shock potential existing in a thin layer and by the upstream $v_i \times B$ force

as in the models by *Lee et al.* [1996] and *Zank et al.* [1996]. *Lembege at al.* [2003] performed hybrid simulations of a perpendicular shock including pickup ions using various treatments of the electrons. They found that when the resistive scale length is resolved electrons are artificially heated when solving the electron energy equation. This artificial electron heating leads to a large potential spike in the ramp which causes shock surfing acceleration.

Particle-in-cell (PIC) simulations of shocks with a 10% relative pickup ion density upstream were performed by *Lee at al.* [2005]. These authors were mainly concerned with the influence of shock reformation on the pickup ion acceleration mechanism: it has been shown by PIC simulations of perpendicular shocks and quasi-perpendicular shocks that such shocks reform on the time scale of the ion gyroperiod. Processes responsible for reformation can be accumulation of specularly reflected ions at the upstream edge of the foot [*Hada et al.* , 2003], instabilities in the foot due to specularly reflected ions [*Scholer et al.* , 2003], or catastrophic steepening of a nonlinear upstream whistler precursor [*Krasnoselskikh et al.* , 2002]. *Lee at al.* [2005] noted that the pickup ions gain in the extended foot a bulk velocity in the y direction perpendicular to the magnetic field (z) and to the shock normal (x). This velocity results, in turn, in a $\mathbf{V}_{PI} \times \mathbf{B}$ electric field in the shock normal direction and thus leads to a modification of the cross-shock potential. The modification of the cross-shock potential in the extended foot by the pickup ions was confirmed in the PIC simulations by *Matsukiyo et al.* [2007]. The authors emphasized the importance of using a realistic ion to electron mass ratio in the PIC simulations. Use of a mass rations less than 400 suppresses the excitation of the modified two-stream instability (MTSI) in the foot of the shock. Furthermore, simulations of an exactly perpendicular shock in a one

spatial dimensional set-up eliminates the occurrence of the MTSI by design: the MTSI has a **k** vector component parallel to the magnetic field **B**, which is not allowed for in 1-D, $\Theta_{Bn} = 90^\circ$ simulations. *Matsukiyo et al.* [2007] furthermore investigated how pickup ions specularly reflected at the ramp gain energy in the y direction during their upstream gyration.

New hybrid simulations with a massless electron fluid with parameters more appropriate to the heliospheric termination shock (25% relative pickup ion density) have recently been presented by *Wu et al.* [2009]. They found that the temperature of cold solar wind ions increases through the shock by a larger factor than that of the pickup ions. However $\sim$ 90% of the downstream pressure is provided by the pickup ions. *Wu et al.* [2010] have analyzed in detail the orbits of pickup ions reflected by the shock. They found that pickup ions can reverse their x component of the velocity just downstream of the shock ramp due to gyration in the enhanced magnetic field of the overshoot. These ions then gain energy by the motional electric field E_y similar to what has been found by *Matsukiyo et al.* [2007].

Matsukiyo et al. [2007] used a relative pickup ion density of only 10%. The Voyager observations indicate a higher pickup ion density of 25% to 30%. We have thus repeated the *Matsukiyo et al.* [2007] simulations with new parameters in order to study 1. the partition of the dissipation energy, 2. the magnitude and the spatial scale of the cross-shock potential, 3. the mechanism/mechanisms of pickup ion reflection, and 4. the percentage of reflected pickup ions relative to the incoming pickup ions. As *Wu et al.* [2009] we model the termination shock in a generic sense rather than reproduce features of Voyager 1 and 2 termination shock crossings. We present results for a 30% relative

pickup ion density. Since, as outlined above, an exactly perpendicular shock in one spatial dimension represents a singularity, we also investigate an oblique shock with $\Theta_{Bn} = 87°$. Furthermore, it is of interest to investigate the transition to a pickup ion dominated shock. We will therefore also present results from simulations of a shock with an upstream relative pickup ion density of 60%. The paper is organized as follows. After a description of the simulation set-up and the shock parameters we first present an overview of an exactly perpendicular shock with 30% pickup ions. We then discuss the magnitude and the spatial scale of the cross-shock potential obtained from various shock simulations with different parameters. Since the potential structure is due to reflected pickup ions we then analyze in detail the reflection process and the reflection rate. It turns out that at not exactly perpendicular shocks including pickup ions the modified two-stream instability is excited in the whole extended foot region and leads to considerable modification of the shock structure. We present a linear instability analysis appropriate for parameters in the foot. Finally we discuss thermalization and partition of the downstream energy gain.

2. Simulation

The shock is produced by the so-called injection method: a high-speed plasma consisting of solar wind electrons, solar wind protons, and pickup protons is injected from the left hand boundary of a one-dimensional simulation system and travels toward positive x. The plasma carries a uniform magnetic field which has a B_z and a B_x component. At the right hand boundary the particles are specularly reflected. A shock then propagates in the $-x$ direction, i.e., the simulation system is the downstream rest frame, and the shock normal is the x axis. Furthermore, the simulations are done in the so-called normal incidence frame where the upstream bulk velocity is parallel to the shock normal. Initially there are

100 particles for each proton species as well as for the electrons in a computational cell. As in earlier work [*Liewer et al.* , 1993], [*Kucharek and Scholer* , 1995], [*Wu et al.* , 2009] the pickup protons velocity distribution is assumed to be a spherical shell comoving with the solar wind, which neglects adiabatic deceleration and velocity space diffusion. Since the shock moves in the simulation system with speed M_s (in units of the Alfvén speed) from the right toward the left the shock Mach number is $M_A = M_o + M_s$ where M_o is the injection velocity of the solar wind. In order to initialize and subsequently inject from the left hand boundary pickup protons for a termination shock simulation M_s has to be known: the pickup protons have to be injected on a sphere in velocity space centered at M_o with radius M_A.

The size of a cell is about one Debye length λ_D ($\Delta x = 0.89\lambda_D$). The computation is done with a total number of 25000 cells corresponding to 1250 electron inertial lengths c/ω_{pe}. In the following, time will be given in units of the inverse of the proton cyclotron frequency Ω_{ci}, distances in units of the electron inertial length λ_e, the velocity in units of the upstream Alfvén speed v_A, magnetic field and the density in units of their upstream values B_0 and n_0, respectively. The potential $e\Phi$ is given in units of $m_i v_0^2/2$, where v_0 is the upstream solar wind velocity relative to the shock. As outlined in the Introduction, we will investigate the low beta case and assume $\beta_i = \beta_e = 0.1$. Because of computational reasons the parameter ω_{pe}/Ω_{ce} is set to 4. In all runs reported here the ion to electron mass ratio is $m_i/m_e = 1024$. Thus the whole system size is ~ 39 ion inertial lengths, λ_i.

We will report in the following results from three different runs. In run A we have assumed that the pickup ion contribution to the upstream density is 30% and that the upstream magnetic field - shock normal angle is $\Theta_{Bn} = 90°$. This value has also been

used by *Wu et al.* [2009] in their simulation. However, as shown already by *Matsukiyo et al.* [2007], slight deviations of Θ_{Bn} from exactly 90° lead to considerable changes in the micro-structure of the shock. We will thus present a second run with a 30% pickup ion density and $\Theta_{Bn} = 87°$ (run B). In order to analyze the transition to a completely pickup ion dominated shock we have increased in a further run C the pickup ion density to 60% ($\Theta_{Bn} = 87°$). The results will be compared with a $\Theta_{Bn} = 90°$ run without a pickup ion contribution (run D). In the runs the injection velocity M_o is assumed to be 4.0. The resulting shocks move in runs A to D with slightly different velocities M_s in the simulation frame to the left hand side. For runs A and B the shock Alfvén Mach number is $M_A \sim 7.3$ and for case C $M_A \sim 8.5$. In run D without pickup ions the shock Alfvén Mach number is $M_A \sim 6.2$.

2.1. Overview

Figure 1 shows for run A in the top panel the magnetic field B_z (solid line) and the potential Φ (broken line). When comparing these results with hybrid simulations it should be remembered that the whole spatial size displayed in Figure 1 is $\sim 16\lambda_i$. The shock ramp is at $\sim 580\lambda_e$ as evidenced by the large increase in the magnetic field. Upstream of the ramp is a small foot produced by specularly reflected solar wind ions and further upstream an extended foot of $\sim 300\lambda_e$ due to the reflected pickup ions corresponding to $\sim 9.3\lambda_i$. Notably is here first the smooth increase of the cross-shock potential over the whole extended foot region with a maximum value of $\sim 0.3 m_i v_0^2/2$. The second panel from top shows gray-shaded the solar wind ion v_{ix} phase space and as a line plot the x component of the pickup ion bulk velocity, V_{px}. The bulk speed of the solar wind ions decreases smoothly in the extended foot and reaches about zero at the ramp; near the

ramp the gray-shaded phase space plot exhibits the existence of the specularly reflected solar wind ions leading to a small foot in the magnetic field. The x component of the pickup ion bulk velocity is over the whole extended foot almost zero (note that these velocities are in the downstream rest frame) indicating that a very large portion of the pickup ions are reflected. In the extended foot the solar wind speed in the normal direction drops gradually from the far upstream value and reaches zero in the downstream frame near the shock ramp. The third panel from top shows gray-shaded the solar wind ion v_{iy} phase space and as a line plot the y component of the pickup ion bulk velocity, V_{py} (y is the direction perpendicular to the shock normal direction and to the magnetic field direction). Clearly visible is the gyration of the specularly reflected solar wind ions in the short foot upstream of the ramp and the large V_{py} in the extended pickup foot due to the gyration of the reflected pickup ions. The bottom panel shows the v_{ex} phase space of the electrons exhibiting an adiabatic increase of the perpendicular velocity of the electrons through the shock.

2.2. Cross-Shock Potential

The cross-field potential responsible for specularly reflecting part of the incoming ions at a perpendicular shock is usually approximated by [*Zank et al.* , 1996]

$$e\Phi \simeq \eta \frac{1}{M_A^2} \frac{\delta B}{B_0} m_i v_0^2 \tag{1}$$

where $\delta B = B_1 - B_0$ is the difference between downstream (1) and upstream (0) magnetic fields and the parameter η has been introduced to approximate the contribution to the shock potential [*Leroy* , 1983] due to the jump in the electron pressure and the V_y bulk

velocity of the reflected ions: the y component of bulk velocity of the reflected ions due to their gyration in the upstream magnetic field leads to an additional electric field term $-V_y B_z$ in the shock normal direction. Usually it is assumed that $\eta \approx 2$; this assumption has also been made recently by *Zank et al.* [2010] when investigating theoretically the microstructure of the heliospheric termination shock. Substituting the difference between downstream and upstream magnetic fields by the shock compression ratio r the normalized (in units of $m_i v_0^2/(2e)$) cross shock potential can then be written as

$$\Phi \simeq 4\frac{(r-1)}{M_A^2} \tag{2}$$

for a weak shock, like the heliospheric termination shock, $r \simeq 2$, so that one would obtain a value of $\Phi \approx 1/16$ for the cross-shock potential $e\Phi$ in units of $m_i v_0^2/2$.

Figure 2 shows the results for the cross-shock potential for all our runs A - D. Shown from top to bottom is the cross shock potential $e\Phi$ in units of $m_i v_0^2/2$ (broken line) versus x from the beginning of the extended pickup ion foot through the shock ramp into the downstream. Also shown for reference is the B_z magnetic field profile. The results for the different runs have been plotted in such a way that the ramp in each case is located at $x = 0$. The top panel shows results for the case without pickup ions (run D), the potential rises in the ramp to a value of 0.55 as expected for a high Mach number shock. The second panel from top shows the profiles for case A. *Matsukiyo et al.* [2007] who reported simulations for a case with 10% pickup ions showed that in this case more than 1/3 of the total potential change occurs in the extended region upstream due to reflected and gyrating pickup ions. As can be seen from the Figure 2, second panel from top, when increasing the pickup ion contribution to 30% the potential increases already in

the extended foot region almost to the maximum value. Moreover, this value is close to 0.35 in units of $m_i v_0^2/2$ and thus by a factor five larger than the value obtained from the approximation given above. For the quasi-perpendicular case (run B) the maximum potential is slightly smaller. In both cases a small increase of the potential is connected with the ramp itself. In the pickup ion dominated case of run C (60% pickup ions) the maximum value of the potential $\sim 0.35 m_i v_0^2/2$ is reached well within the extended foot region produced by the reflected pickup ions. The deviation of the cross shock potential structure and magnitude in the case of weak shocks with a large upstream pickup ion contribution from the simple approximation given above is due the neglect of the large contribution to the potential by the term involving the y component of the reflected and gyrating pickup ions.

2.3. Pickup Ion Reflection and Energy Gain

The reflection of pickup ions at a perpendicular shock is important for the subsequent pickup ion energy gain. At a supercritical shock part of the incoming solar wind ions are specularly reflected by the normal electric field E_x and by the increase in the magnetic field B_z in the ramp. In this process the v_{ix} velocity is reversed in a time short with the ion gyroperiod without any larger change of the very small v_{iy} component. The specularly reflected ions begin to gyrate in the foot upstream of the ramp and gain energy when moving in the y direction by the motional electric field $V_x \times B_z$. The reflected ions are accelerated up to twice the solar wind velocity and eventually gyrate downstream where they contribute to the downstream heating. *Matsukiyo et al.* [2007] have analyzed analytically the orbit of a pickup ion which is specularly reflected at a shock. They have determined the gyrophase at shock encounter of those pickup ions which, after specular re-

flection, spend the maximum time during the upstream gyration before being transmitted again downstream. These reflected pickup ions will gain during their upstream gyration energies considerably larger than the specularly reflected solar wind ions. *Matsukiyo et al.* [2007] have estimated the maximum kinetic energy gain ϵ of specularly reflected pickup ions to be ~ 14 times the energy of the solar wind ϵ_{in}, where ϵ_{in} is in the downstream rest frame (simulation frame).

Using hybrid simulations of a perpendicular shock the reflection process of pickup ions has been investigated in detail by *Wu et al.* [2010]. They found that the places where the x velocity of a pickup ion changes sign from positive to negative is widely dispersed in the vicinity of the shock. Those reflected ions which reverse the x direction close but downstream of the ramp gain higher energies than those reversing the direction upstream of the ramp or further downstream. The present simulations have basically confirmed this picture. We should like to add a few points. *Wu et al.* [2010] have emphasized that the pickup ions are not specularly reflected, but that rather the x velocity is reversed downstream of the ramp due to gyration in the enhanced magnetic field in the overshoot. The argument is basically based on the assumption that in specular reflection v_y should stay constant while v_x rapidly changes sign, which they did not see in their simulation. Figure 3 shows results from run B. Shown is color-coded in the top panel the magnetic field B_z as a function of time t and x. Time is here in units of the inverse ion gyrofrequency. In the downstream rest frame the shock (yellow-red color) moves with increasing time to the left. Also indicated is the trajectory of a pickup ions which is reflected by the shock. As in *Wu et al.* [2010] this pickup ion is not reflected in the ramp but in the magnetic field overshoot. The lower left hand panel shows the orbit of the reflected pickup ion in

v_{iy} - v_{ix} velocity space. Zero x velocity is the downstream rest frame (simulation frame) and the velocities are in units of the injection velocity V_{in} of the ions at the left hand site of the simulation system. Tick marks on the orbit are equidistant in time. Initially the orbit is in the shock frame a circle centered at the solar wind velocity with a radius equal to solar wind velocity; in the downstream rest frame this circle is shifted to the left of the $v_x = 0$ line. The zero v_x velocity in the shock frame is indicated by a dashed line. As the ion reaches the high magnetic field in the overshoot with a negative velocity v_{iy} the orbit becomes rapidly changed: within less than 0.1 of the gyroperiod the velocity v_{ix} changes sign in the shock frame of reference, i.e. the orbit crosses the dashed line, while the velocity v_{iy} stays negative and is almost constant. Having a negative velocity v_x the ion moves upstream away from the shock. It continues the gyration and once the v_y velocity becomes positive the particle gains energy in the positive motional electric field E_y upstream. The energy gain can be seen from the upper right hand panel. Shown is the energy of the ion in the two components v_{ix} (blue) and v_{iy} (red) and the total energy ϵ. Two sets of arrows indicate times corresponding to arrows on the orbit in the v_{ix} - v_{iy} plane. The total energy increases in the region upstream when the pickup ion moves with positive v_{iy} in the direction of positive E_y. This is similar to what has been found by *Wu et al.* [2010] by hybrid simulations. *Wu et al.* [2010] have suggested that pickup ions gain negative v_x not by specular reflection, but by the large scale gyromotion. Based on the fact that the change of the velocity from shock directed to upstream directed occurs in a time very short compared with the gyroperiod and without considerable change in v_y it seems that the reflection process is nevertheless nearly specular. Reflection is due to the nonadiabatic orbit change when the pickup ion enters the strong magnetic field of

the overshoot. The pickup ion trajectories are controlled by the shock B_z and E_x fields and the motional electric field E_y, so that the Lorentz force components in the $\hat{x}$ and $\hat{y}$ directions are

$$\mathbf{F} = q(E_x + v_y B_z)\hat{x} + q(E_y - v_x B_z)\hat{y} \tag{3}$$

where $E_y = v_0 B_z$. In specular reflection of part of the incoming solar wind ions v_y is small, thus reflection is mainly due to the large negative E_x force in the negative x direction in the shock. However in the case of pickup ions almost half of the distribution has a large negative v_y component; the large B_z value in the overshoot results in a large negative Lorentz force $v_y B_z$ turning these pickup ions into the upstream $(-\hat{x})$ direction. Figure 4 shows the orbit of a pickup ions reflected in the overshoot in the $v_y - x$ (top panel) and in the $y - x$ plane. Before reaching the overshoot the ion exhibits in the $y - x$ pane the characteristic cusp shaped orbit. It reaches the overshoot with a negative velocity v_y and the magnetic field force reflects the ion.

We should like to point out already here the small scale structures in the extended foot in front of the ramp, which can be seen from the color-coding of the magnetic field in the left hand panel of Figure 3. These structures occur when the magnetic field - shock normal angle deviates from 90° and are due to instabilities in the foot as will be discussed later.

Only one part of the pickup ions are reflected by the magnetic field in the overshoot. Figure 5 shows results from run C with a pickup ion contribution of 60%. In the top two panels are shown by color-coded phase space plots v_{ix} versus x and v_{iy} versus x of the pickup ions at one particular time. Also shown by red is the solar wind ion phase space.

Indicated by two lines is the pickup ion bulk velocity (black line) and the solar wind ion bulk velocity (white line). The V_{py} bulk velocity of the pickup ions increases from upstream in two steps. The color coding of the v_{ix} - x and v_{iy} - x phase space plots shows that the reflected pickup ions consist upstream of two different populations which extend like two different tongues toward upstream. The most upstream part of population 1 is indicated by a white box, the upstream region of population 2 is indicated by a black box. Ions in these boxes in phase space have been followed in time during the run. The result is shown in the lower panel of Figure 5. Shown is here color-coded the magnetic field B_z in the t - x plane. Superimposed are pickup ion trajectories from ions ending in the back box (black lines) and of ions ending in the white box (white lines). The time when the phase space plots in the upper two panels where plotted is indicated in the lower panel by a dashed black line. It can be seen that ions in the two different tongues in phase space have different histories: those ions in the black box have been reflected in the magnetic field overshoot (black trajectories), ions in the white box have been turned around in the extended foot region by the large potential increase. However, the reflection point is also for these ions determined by the occurrence of a negative v_y during the orbit. Figure 6 shows the trajectory of one of the ions reflected in the extended foot in the same format as Figure 4. At the point where the ion turns back upstream the velocity component v_y is negative. Both, the electric and the magnetic term of the Lorentz force component $F_x = q(E_x + v_y B_z)$ contribute in reversing the direction.

An important number is the ratio of reflected and transmitted pickup ions. This number depends somewhat on the definition of reflection. The criterion we have used is as follows. From a time t^* trajectories of all particles in the extended foot, i.e., between the upstream

edge and the overshoot, are traced backward in time. For each particle the number of times I the particle changes the sign of the v_x velocity in the shock frame is determined until the particle is upstream of the extended foot. A particle has been defined reflected if either of the following conditions is satisfied (1) $I \geq 2$ if $v_x > 0$ at $t = t^*$ or (2) $I \geq 1$ if $v_x < 0$ at $t = t^*$. The reflection ratio is defined as $R = N_{ref}/N_{in}$, where N_{ref} and N_{in} are number densities of reflected and injected pickup ions. For run B (30% pickup ions) we find that $R = 0.92$ and for run C (60% pickup ions) we find that $R = 0.84$, i.e., almost all pickup ions are reflected. The fact that almost all pickup ions are reflected is the reason that the pickup ion bulk velocity in the extended foot is zero. Since this velocity is taken in the simulation frame, i.e., in the downstream rest frame, the pickup ion bulk velocity in the foot is essentially equal to the bulk velocity downstream of the foot.

2.4. Modified Two-Stream Instability

Most simulations which including pickup ions have been done for an exactly perpendicular shock. *Matsukiyo et al.* [2007] have shown that if the upstream magnetic field - shock normal angle deviates from 90° and thus k vector components of instabilities parallel to the magnetic field are allowed for the modified two-stream instability can get excited and leads to considerable shock modification. Although the termination shock is expected to have a value of Θ_{Bn} close to 90° an exactly perpendicular shock is a singularity. Voyager 2 data have actually resulted in $\Theta_{Bn} = 82.8° \pm 3.9°$ for the second shock crossing and in $\Theta_{Bn} = 74.3° \pm 11.2°$ for the third termination shock crossing, respectively. We have used in runs B and C a value of $\Theta_{Bn} = 87°$. Figure 7 shows a comparison between the 30% pickup ions run for $\Theta_{Bn} = 90°$ (run A) and for $\Theta_{Bn} = 87°$ (run B). Shown is the magnetic field component B_z stacked in time; time runs from bottom to top. In the $\Theta_{Bn} = 90°$

case (top panel) one can see the magnetic field increase in the foot and the well-defined shock ramp. The shock is reforming itself due to the presence of specularly reflected solar wind ions. The reformation leads to a temporarily steeper and flatter shock ramp. During times of a steep ramp the ramp scale length L is about $L \sim 4\lambda_e$, i.e., considerably smaller than the ion inertial length ($\lambda_e = 0.031\lambda_i$). Thus the assertion of *Wu et al.* [2009] that with the adding of pickup ions to the termination shock the ramp should widen is not correct. In the $\Theta_{Bn} = 87^\circ$ case (bottom panel) the magnetic field profile exhibits small wavelengths waves halfway through the extended foot and reformation has disappeared.

We will argue in the following that the small scale structures are due to the modified two-stream instability (MTSI). Figure 8 shows for run B various quantities at one particular time versus shock normal direction in the same format as in Figure 1. Small-scale wavelengths wave are superimposed on the B_z profile and the incoming solar wind exhibits vortices in v_{ix} - x phase space. These vortices result via phase mixing in a temperature increase of the solar wind ions upstream of the ramp. The electrons exhibit vortices in v_z - x phase space which leads to a large electron temperature parallel to the magnetic field well before the ramp. The excitation of the MTSI is due to the fact that the electrons are decelerated relative to the solar wind protons; the resulting velocity difference $v_{ex} - v_{ix}$ leads to the excitation of the instability. The instability itself does not directly involve the pickup ions, rather the low bulk velocity V_{px} of the pickup ions in the extended foot results in a reduction of the electron bulk velocity. This assumes that the total electrical current in the shock norma direction is zero. As far as the MTSI is concerned the reflected pickup ions take thus over the role of the specular reflected ions at shocks with no pickup ions. Thus the MTSI is excited over the whole extended foot region.

We have solved the linear dispersion relation for a situation appropriate to the conditions in the extended foot region. It was assumed that there is zero electrical current in the shock normal direction and that the bulk velocity difference between the solar wind ions and the pickup ions in the x direction is $V_{xsw} - V_{xp} = 2$. Since the magnetic field increases in the extended foot we have calculated the growth rate for different Θ_{Bn} values. For the instability analysis it is assumed that there are three components: solar wind ions, pickup ions and solar wind electrons, which are all represented by drifting Maxwellians. The thermal velocity of the pickup ions is assumed to be equal to v_0. Figure 9 shows the growth rate γ/Ω_{ci} of the MTSI as function of k for different angles Θ_{Bn}. The upper panel shows the result for the 30% pickup ion case and the lower panel shows the result for the 60% pickup ion case, respectively. No curves for $\Theta_{Bn} = 88°$ or $\Theta_{Bn} = 89°$ means that the growth rate is below $\gamma/\Omega_{ci} = 0.1$ or negative. As can be seen from Figure 9 the growth rates for the MTSI near $\Theta_{Bn} = 87°$ are positive and the wavelength at maximum growth is at $\sim 6\lambda_e$, which is consistent with the wavelengths of the waves in the extended foot. This suggests that the perpendicular heating of the solar wind ions and the parallel heating of the solar wind electrons before they reache the ramp is due to the MTSI. *Matsukiyo et al.* [2007] have shown that reformation of quasi-perpendicular shocks with no pickup ions depends on the solar wind ion beta. For high solar wind ion beta the velocity difference between the incoming solar wind ions and the specularly reflected ions is close to the thermal ion velocity so that they are not well separated in v_x. This has the effect that the ramp widens and reformation ceases. Pre-heating of the solar wind ions in the extended foot by the MTSI in the oblique shock simulation is likely to be the reason

for suppression of the reformation process. The minimum shock ramp scale in the oblique case is $L \sim 24\lambda_e = 0.75\lambda_i$.

Figure 10 shows results for the 60% pickup ion case (run C) in the same format as Figures 1 and 8. The cross-shock potential (broken line in the upper panel) reaches the maximum value in the extended pickup ion foot and decreases toward the magnetic field overshoot. The lower part of Figure 10 shows grey-shades a blow up of the solar wind ion phase space v_{ix} (solid line is the pickup ion bulk speed) and of the solar wind electron phase space v_{ez} over a region of $100\lambda_i$ in the foot. From the vortices in both phase space representations it can be seen that the MTSI is also excited in this higher relative pickup ion densoty case, although with smaller amplitudes.

2.5. Thermalization and Energy Partition

Figures 11 shows (from top to bottom) the electron temperature T_e, the solar wind ion temperature T_{sw}, the pickup ion temperature T_{PI}, the temperature $\sum T$ defined by $n_{sw}T_{sw} + n_{PI}T_{PI} + n_eT_e$, and the solar wind ion n_{sw} and pickup ion density n_{PI} (in units of the upstream electron density), respectively, versus x near the end of run B. The temperatures are in units of $m_iv_0^2$ and the densities are in units of the upstream electron density. The position of the shock ramp can be seen from the overshoot in the solar wind ion temperature. The temperatures in the two top panels demonstrate the heating of the electrons and the pre-heating of the solar wind ions by the MTSI. Almost all electron heating is due to the MTSI and the solar wind ions are pre-heated in the foot by a factor $T_u^{sw}/T_{foot}^{sw} \sim 4-5$, where T_u^{sw} is the upstream solar wind ion temperature and T_{foot}^{sw} is the solar wind ion temperature in the foot close to the ramp. The main solar wind thermalization occurs through the ramp and the temperature reaches an almost constant

level downstream of the overshoot. The ratio of downstream to upstream solar wind ion temperature is $\tau_{sw} = T_d^{sw}/T_u^{sw} \sim 14.4$, which is close to the value of 10 observed by Voyager 2, but smaller than the value of ~ 43 obtained from hybrid simulations by *Wu et al.* [2010]. We note that in the $\Theta_{Bn} = 87°$ case there are very few specularly reflected solar wind ions (as opposed to the $\Theta_{Bn} = 90°$ case) so that solar wind ion heating is mainly due to adiabatic compression after pre-heating by the MTSI. The pickup ion thermalization occurs in the extended foot region and is completed when reaching the ramp. Comparison of the temperature $\sum T$ with the pickup ion temperature indicates that pickup ion heating accounts for almost all of the dissipation. This can be quantified as follows.

The percentage of thermal energy η_j gained by the ion/electron population j can be written [*Wu et al.* , 2010] as

$$\eta_j = n_j \frac{T_d^j - T_u^j}{\sum_{k=sw,PI,e} n_k (T_d^k - T_u^k)} \tag{4}$$

where j can be the pickup ions (PI), the solar wind ions (sw), and the electrons e respectively. We obtain for run A $\eta_{PI} \approx 0.91$, i.e. $\sim 91\%$ of the net energy gain through the shock goes into pickup ions. Furthermore, $\eta_{sw} \approx 0.08$ and $\eta_e \approx 0.01$, i.e., $\sim 8\%$ goes into the solar wind ions and $\sim 1\%$ into electrons, respectively. It should be noted that in the present PIC simulations the downstream region, i.e., the region between the overshoot and the right hand reflecting wall, is still rather limited and $\sim 20\lambda_i$. This has to be contrasted with a region of $\sim 100\lambda_i$ in hybrid simulations [*Wu et al.* , 2009]. The temperature in this limited region behind the overshoot has not yet reached a steady level. For run B we obtain $\eta_{PI} \approx 0.885$, $\eta_{sw} \approx 0.090$, and $\eta_e \approx 0.025$, respectively. It can be seen that the thermal energy gain of the electrons in this oblique shock is more than twice as

much as compared to the exactly perpendicular shock, which is due to the occurrence of the MTSI. Another measure for the energy partition is the downstream thermal pressure in the pickup ions relative to the total downstream pressure, $\chi_d = (P_d^{PI}/P_d)$. The pressure ratio in the region of $\sim 20\lambda_i$ behind the overshoot varies between 0.82 and 0.92 and is consistent with the energy fraction gain of 84% for pickup ions as inferred by V2 observations [*Richardson* , 2008].

Figure 12 shows results for run C (60% pickup ions) in the same format as Figure 10. The electron temperature increases continuously due to adiabatic compression in the extended foot and reaches at the ramp almost the downstream value. Downstream electron temperature spikes are due to the large magnetic field spikes from the large-amplitude MTSI waves downstream of the ramp (see Figure 2). The solar wind ion temperature increases slightly in the ramp due to adiabatic compression. In the bottom panel one can see clearly a two step increase of the pickup ion density due to the two different reflection processes in the ramp/overshoot and in the upstream part of the extended foot. In the 60% pickup ion case we obtain for the percentage of thermal energy gained by the pickup ions $\eta_{PI} \approx 0.96$.

3. Summary and Discussion

The results of the PIC simulations presented above can be summarized as follows.

1. Upstream of the ramp is an extended foot due to reflected pickup ions. In this foot the magnetic field continuously increases and the bulk speed of the solar wind ions decrease and reach at the magnetic field ramp the downstream value. The bulk speed of the pickup ions, V_{px}, is zero (in the downstream rest frame) over almost the whole extended foot region. However, the pickup ions have in this extended foot a large (of the

same order as the upstream solar wind bulk velocity) positive bulk velocity component V_{py} perpendicular to the shock normal and to the magnetic field. This is due to the gyration of the reflected pickup ions and their subsequent acceleration by the motional $\mathbf{V} \times \mathbf{B}$ electric field in the y direction.

2. The positive V_{py} bulk velocity of the pickup ions in the extended foot causes a $-V_{py}B_z$ electric field in the x direction. This leads to an increase of the shock potential upstream of the magnetic field ramp. A first maximum of the potential is reached within the foot. The potential then decreases toward the ramp where it has a second maximum of about the same magnitude as the first maximum. The maximum value of the potential is $\sim 0.35 m_i v_0^2/2$ and is by a factor ~ 5 larger than expected for a weak shock without pickup ions. The potential jump near the ramp is $\sim 0.07 m_i v_0^2/2$ (30% pickup ions relative density).

3. The process of pickup ion reflection can be separated into two different mechanisms. Pickup ions which reach the magnetic field overshoot with a negative v_y velocity component are magnetically deflected by the negative $v_y B_z$ Lorentz force term. This leads to specular reflection with a change in the sign of v_x while v_y stays constant. Pickup ions which have a negative v_y within the extended foot are turned upstream by a combination of magnetic reflection and the upstream directed (negative) electric field E_x. For a shock with a pickup ion relative density of 30% the reflection rate is 92%, for a shock with a pickup ion relative density of 60% the reflection rate is 84%.

4. In the 30% pickup ion case and for an exactly perpendicular shock 91% of the total thermal energy gain in the shock is gained by pickup ions, 8% by the solar wind ions, and 1% by electrons. The thermal energy gain by pickup ions increases as the pickup ion

relative density increases. The pickup ion temperature increases continuously from the upstream edge of the extended foot to the shock ramp and stays then constant through the overshoot and downstream. Conversion of upstream bulk energy into thermal energy of pickup ions is the main dissipation mechanism in shocks with a high pickup relative density and is completed when the pickup ions reach the shock.

5. The exactly perpendicular shock with a 30% relative pickup ion density exhibits reformation due to specularly reflected solar wind ions. The ramp scale varies and can be as small as several ~ 4 times the electron inertial length. Thus addition of pickup ions does not lead to a shock widening nor is reformation inhibited. In the $\Theta_{Bn} = 87°$ case the modified two-stream instability is excited in the extended foot region. The free energy of the instability is the bulk velocity difference between solar wind ions and solar wind electrons: due to the reflected pickup ions the solar wind electron bulk speed has to decrease relative to the bulk speed of the solar wind ion when requiring zero electrical current. The MTSI leads to pre-heating of the solar wind ions perpendicular to the magnetic field and to electron heating parallel to the magnetic field. Most of the electron heating through the shock is due to the MTSI upstream of the shock ramp. The pre-heating of the solar wind ion in the extended foot inhibits shock reformation and leads to a widening of the shock ramp.

Conversion of bulk motional energy into thermal energy in a pickup ion loaded shock (above 30% relative pickup ion density) is mainly through acceleration of reflected pickup ions by the motional electric field in the extended foot during their upstream gyration. This results in a large pickup ion bulk speed perpendicular to the magnetic field and perpendicular to the shock normal. This bulk speed, in turn, leads to an electric field

in the shock normal direction with the result that the shock potential increases in the extended foot to a value comparable to the ion ram energy. This potential increase in the extended foot decelerates the solar wind and is partly responsible for reflecting the pickup ions within the foot. The slowing down of the solar wind results in a smaller motional electric field, which, however is needed: with the high reflection rate of pickup ions the far upstream motional electric field would lead to too large pickup ion acceleration.

When constructing analytical or semi-analytical models for pickup ion loaded shocks all these ingredients have to be taken into account. It is certainly possible to construct models with small pickup ion reflection rates and have these gain large energies during their upstream gyration so that they carry most of the downstream pressure, but such models do probably not reflect reality. We note further that slight variations from an exactly perpendicular shock to more oblique shocks lead to instabilities in the foot which may drastically change the reflection and thermalization processes. This is particularly true for one-dimensional simulations which allow only for $\mathbf{k}$ vectors in the shock normal directions. Thus 1-D simulations of an exactly perpendicular shock exclude by design foot instabilities. Instabilities, like the modified two-stream instability obtained here in the $\Theta_{Bn} = 87°$, 30% relative pickup ion density case, are more important in pickup ion loaded shocks than in shocks without pickup ions: in the extended foot the instabilities can have sufficient time to grow to nonlinear amplitudes before they are swept into the shock.

Our simulations agree in many aspects with the hybrid simulations by *Wu et al.* [2009] and *Wu et al.* [2010]. In particular *Wu et al.* [2010] found that the pickup ions are reflected in the magnetic field overshoot. We obtain the same type of reflected orbits in the present PIC simulations. However, since the transverse velocity component during

magnetic reflection in the overshoot is almost constant reflection can be considered as being specular. As *Wu et al.* [2010] we find that although the temperature of cold solar wind ions increases through the shock by a larger factor than that of the pickup ions, $\sim$ 90% of the downstream pressure is provided by the pickup ions. In contrast to the assumption by *Wu et al.* [2010] that due to the pickup ions the ramp widens we obtain during the reformation cycle of an exactly perpendicular shock in the 1-D simulation ramp scales of a few electron inertial length. This is a non-realistic result in the sense that as soon as an off 90° Θ_{Bn} is allowed for the modified two-stream instability leads to a pre-heating of the solar wind and to a ramp widening.

In a semi-analytical model *Zank et al.* [2010] have assumed that the cross shock potential is small (1/16 in units of the ram energy) and those pickup ions are reflected which have a velocity (in the shock frame) smaller than 1/4 of the shock speed. This is at variance with the present simulations: not only is the structure of the potential very different from that of a shock without pickup ions, but the magnetic field force term of the Lorentz force is the most important term for ion reflection. The *Zank et al.* [2010] model considerably underestimates the reflection rate of pickup ions and overestimates the energy the reflected pickup ions gain before being transmitted downstream. Overestimation is due to the fact that the bulk flow speed into the shock is decreases in the extended foot toward the ramp, so that the energy gain by the motional electric field per pickup ion is smaller. We found that both, the bulk velocity of the solar wind ions and the bulk velocity of the pickup ions, decreases in the extended foot well before the ramp to the downstream value. The motional electric field is thus near the ramp considerably smaller than in the upstream solar wind. Models for acceleration of pickup ions to higher energies by

shock drift have to take this into account. For example *Yang et al.* [2009] have followed pickup ions as test particles in magnetic and electric fields issued from (not self-consistent) PIC simulations of shocks in order to study drift and surfing acceleration of these ions. While such computations are interesting, they have probably only limited relevance for the acceleration process of pickup ions at the termination shock.

In the present simulations the plasma is still strongly magnetized since a value of $\omega_{pe}/\Omega_{ce} = 4$ has been used. The low value of ω_{pe}/Ω_{ce} may result in an overestimation of the role of the electric field for particle dynamics. The present simulations are one dimensional in space. The one-dimensionality may overemphasize the amplitude of the MTSI waves since a rather limited region of $\mathbf{k}$ space is available. Furthermore if a higher spatial dimensionality is allowed, other instabilities with different $\mathbf{k}$ vectors relative to the magnetic field are most probably excited [*Matsukiyo and Scholer* , 2006].

Acknowledgments. M. S. is grateful for Fellowship of the Japanese Society for the Promotion of Science. S. M. is supported by a Grant-in-Aid for Young Scientists (B) No. 22740323 from JSPS.

References

Burlaga, L. F., N. F. Ness, M. H. Acuna, R. P. Lepping, J. E. Connerney, E. C. Stone, and F. B. McDonald (2005), *Science*, *309*, 2027, doi:10.1126/science.1117542.

Burlaga, L. F., N. F. Ness, M. H. Acuna, R. P. Lepping, J. E. Connerney, and J. D. Richardson (2008), Magnetic fields at the solar wind termination shock ,*Nature*, *454*, 75, doi:10.1038/nature07039.

584 Decker, R. B., S. M. Krimigis, E. C. Roelof, M. E. Hill, T. P. Armstrong, G. Gloeckler,
585 D. C. Hamilton, and L. J. Lanzerotti (2008), Mediation of the solar wind termination
586 shock by non-thermal ions,*Nature*, *454*, 67, doi:10.1038/nature07030.
587 Hada, T., M. Oonishi, B. Lembège, and P. Savoini (2003), Shock front nonsta-
588 tionarity of supercritical perpendicular shocks, J. Geophys. Res., 108 (A16), 1233,
589 doi:10.1029/2002JA009339.
590 Krasnoselskikh, V. V., B. Lembège, P. Savoini, and V. V. Lobzin (2002), . Nonstationarity
591 of strong collisionless quasiperpendicular shocks: Theory and full particle simulations,
592 Phys. Plasmas, 9, 1192.
593 Kucharek, H., and M. Scholer (1995), Injection and acceleration of interstellar pickup ions
594 at the heliospheric termination shock, *J. Geophys. Res., 100*, 1745.
595 Lee, M. A., V. D. Shapiro, and R. Z. Sagdeev (1996), Pickup ion energization by shock
596 surfing, *J. Geophys. Res., 101*, 4777.
597 Lee, R. E., S. C. Chapman, and R. O. Dendy (2005), Reforming perpendicular shocks in
598 the presence of pickup protons: initial ion acceleration, *Ann. Geophys., 23*, 643.
599 Lembege, B., J. Giacalone, M. Scholer, T. Hada, M. Hoshino, V. Krasnoselskikh, H.
600 Kucharewk, P. Savoini, and T. Teraswa (2003), Selected problems in collisionless shock
601 physics, *Space Sc. Rev., 110*, 161.
602 Leroy, M. M. (1983), Structure of perpendicular shocks in collisionless plasmas, *Phys.
603 Fluids, 26*, 2742.
604 Liewer, P. C., B. E. Goldstein, and N. Omidi (1993), Hybrid simulations of the effects of
605 interstellar pickup hydrogen on the solar wind termination shock, *J. Geophys. Res., 98*,
606 15,211.

Lipatov, A. S., and G. P. Zank (1999), Pickup ion acceleration at low β_p perpendicular shocks, *Phys. Rev. Lett., 82*, 3609.

McComas, D. J., *et al.* (2009), Global observations of the interstellar ineraction from thze interstellar boundary , *Science*, *326*, 2017, doi:10.1126/science.1180906.

Matsukiyo, S. and M. Scholer (2006), On microinstabilities in the foot of high Mach number quasi-perpendicular shocks, *J. Geophys Res.,* 111 (A06104), doi:10.1029/2005JA011409.

Matsukiyo, M. Scholer, and D. Burgess (2007), Pickup ions at quasi-perpendicular shocks: full particle electrodynamic simulations, *Ann. Geophys., 25*, 283.

Richardson, J. D. (2008), Plasma temperature distributions in the heliosheath,*Geophys. Res. Lett.*, *35*, L23104, doi:10.1029/2008GL036168.

Richardson, J. D., J. C. Kasper, C. Wang, J. W. Belcher, and A. J. Lazarus (2008), Cool heliosheth plasma and deceleration of the upstream solar wind at the termination shock,*Nature*, *454*, 63, doi:10.1038/nature07024.

Scholer, M., Shinohara, I., and S. Matsukiyo (2003), Quasi-perpendicular shocks: Length scale of the cross-shock potential, shock reformation, and implication for shock surfing, J. Geophys. Res., 108 (A1), 1014, doi:10.1029/2002JA009515.

Stone, E. C., A. C. Cummings, F. B. McDonald, B. C. Heikkila, N. Lal, and W. R. Webber (2005), Voyager 1 explores the termination shock region and the heliosheath beyond, *Science*, *309*, 2017, doi:10.1126/science.1117684.

Wu, P., D. Winske, S. P. Gary, N. A. Schwadron, and M. A. Lee (2009), Energy dissipation and ion heating at the heliospheric termination shock, *J. Geophys. Res., 114*, A08103, doi:10.10292009JA014240.

630 Wu, P., K. Liu, D. Winske, S. P. Gary, N. A. Schwadron, and H. O. Funsten (2010),
631 Hybrid simulations of the termionation shock: Suprathermal ion velocity distributions
632 in the heliosheath, *J. Geophys. Res.,* in press.
633 Yang, Z. W., Q. M. Lu, B. Lembege, and S. Wang (2009), Shock front nonstationarity and
634 ion acceleration in supercritical perpendicular shocks, *J. Geophys. Res., 114*, A03111,
635 doi:10.10292008JA013785.
636 Zank, G. P., H. L. Pauls, I. H. Cairns, and G, M. Webb (1996), Interstellar pickup ions
637 and quasi-perpendicular shocks: Implications for the termination shock, *J. Geophys.*
638 *Res., 101*, 457.
639 Zank, G. P., J. Heerikshuisen, N. V. Pogorelov, R. Burrows, and D. McComas (2010),
640 Microstructure of the heliospheric termination shock: Implications for energetic neutral
641 atom observations, *Astrophys. J., 708*, 1092.

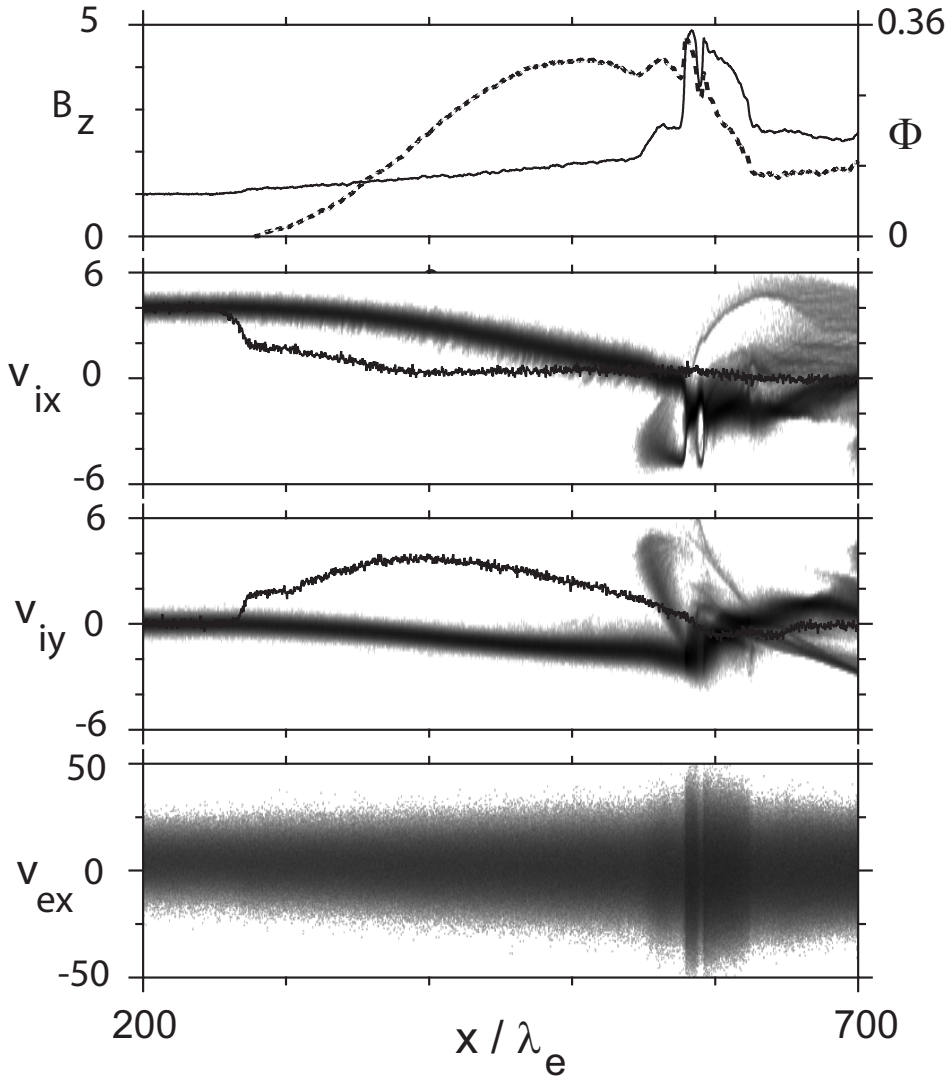

Figure 1. Results for run A. From top to bottom: Magnetic field B_z component (solid line) and cross shock potential (broken line), solar wind ion v_{ix} phase space (grey) and pickup ion bulk velocity component v_{px} (solid line), solar wind ion v_{iy} phase space (grey) and pickup ion bulk velocity component v_{py} (solid line), and solar wind electron phase space v_{ex} versus shock normal direction x.

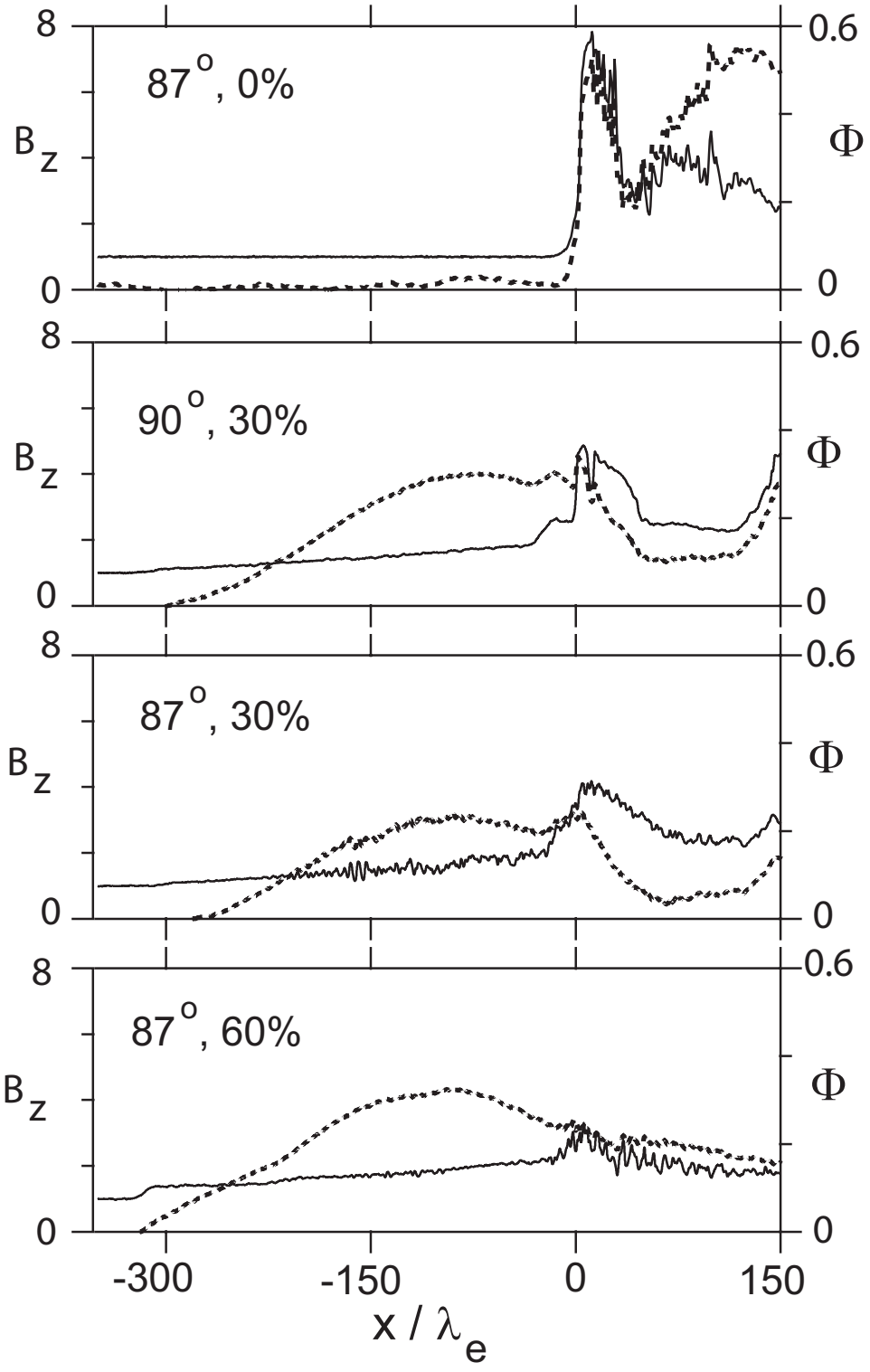

Figure 2. Magnetic field B_z component (solid line) and cross shock potential (broken line) versus shock normal direction x for all runs. In each panel is given the magnetic field - shock normal angle Θ_{Bn} and the percentage of pickup ions in the respective run.

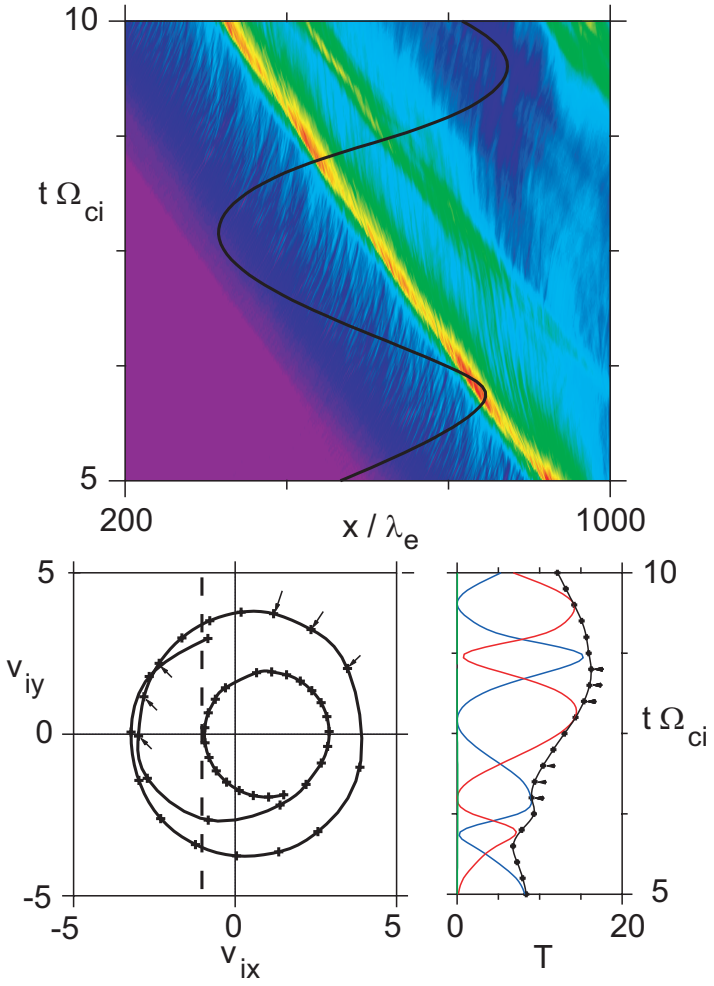

Figure 3. Top: Color coded magnetic field B_z component in the $t - x$ plane. The shock overshoot can be seen as a red/yellow band. The shock is moving into the positive x direction since the presentation is in the downstream rest frame. Also shown is the trajectory of a pickup ion reflected in the overshoot. Bottom left: Trajectory of the reflected pickup ion in the $v_y - v_x$ plane (velocities are in the downstream rest frame; the broken line indicates the position of the shock frame). Bottom right: Energy T of the reflected pickup ion versus time. Black line is total energy, red line and blue line are energies in the v_y and v_x components, respectively

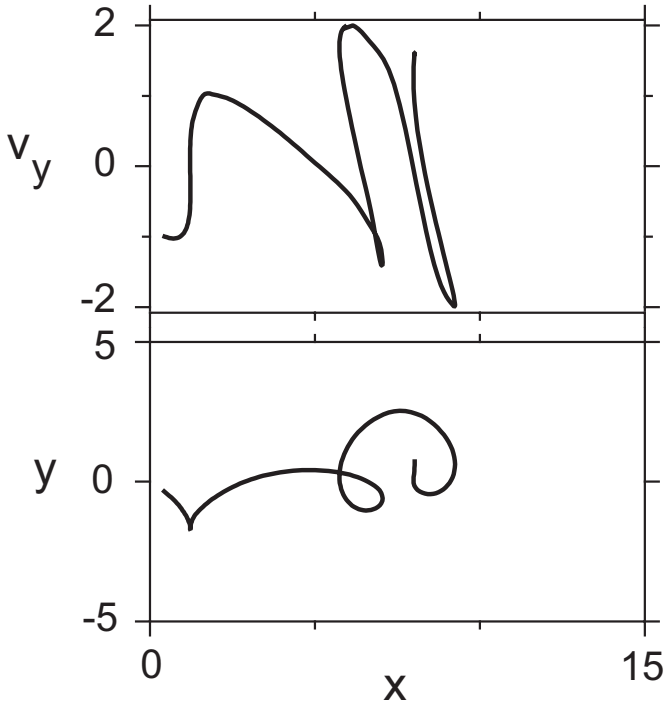

Figure 4. Trajectory of a pickup ions which is reflected in the magnetic field overshoot in the $v_y - x$ (top) and $y - x$ planes.

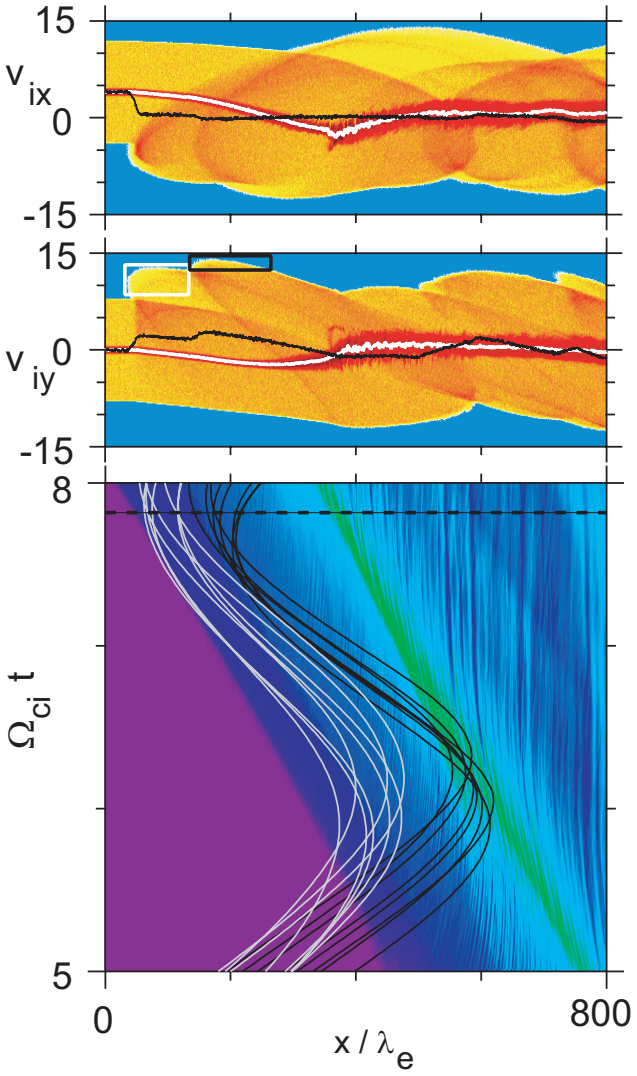

Figure 5. Top two panesl: color-coded $v_{ix} - x$ and $v_{iy} - x$ phase space plots of pickup ions (yedllow - orange) and solar wind ions (red). Black line are the pickup ion bulks velocity components, white lines are the solar wind bulk velocity components. Bottom panel: Color coded magnetic field B_z component in the $t - x$ plane (in the downstream rest frame. The time where the phase space densities in the two top panels are shown is indicated by a dashed horizontal line. Also indicated are trajectories of pickup ions which are sampled at this time in the two white and black boxes in $v_y - x$ phase space, respectively.

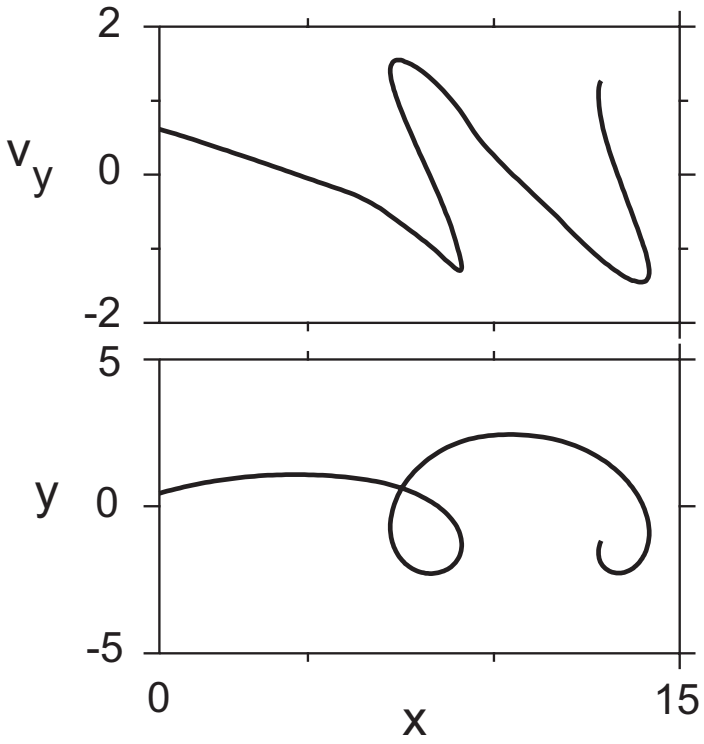

Figure 6. Trajectory of a pickup ions (white trajectory in Figure 5, bottom panel) which is reflected in the extended foot in the $v_y - x$ (top) and $y - x$ planes.

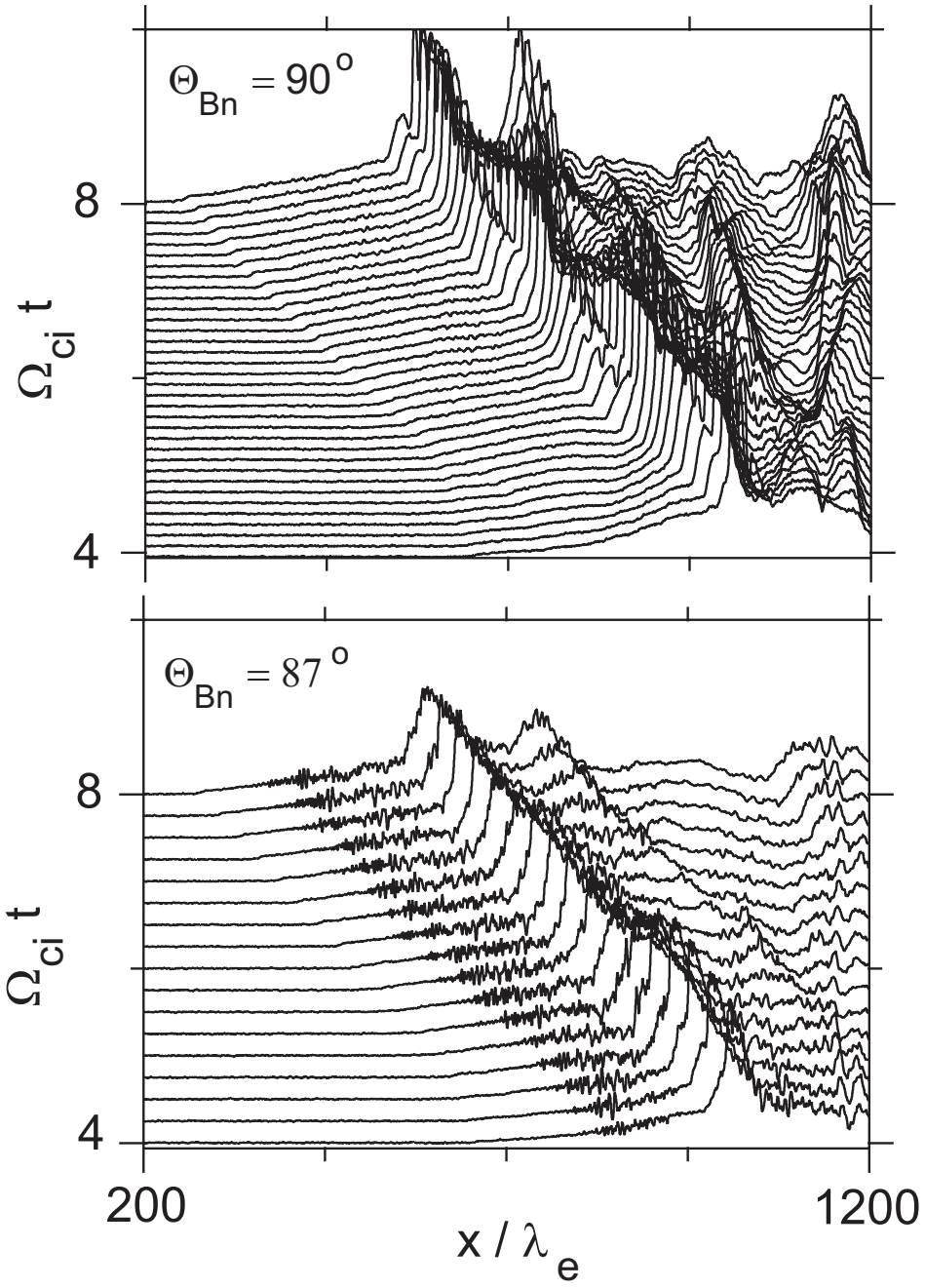

Figure 7. Comparison between the 30% pickup ions run for $\Theta_{Bn} = 90°$ (run A) (top panel)and for $\Theta_{Bn} = 87°$ (run B) (bottom panel). Shown is the magnetic field B_z component stacked in time in the downstream (simulation) frame.

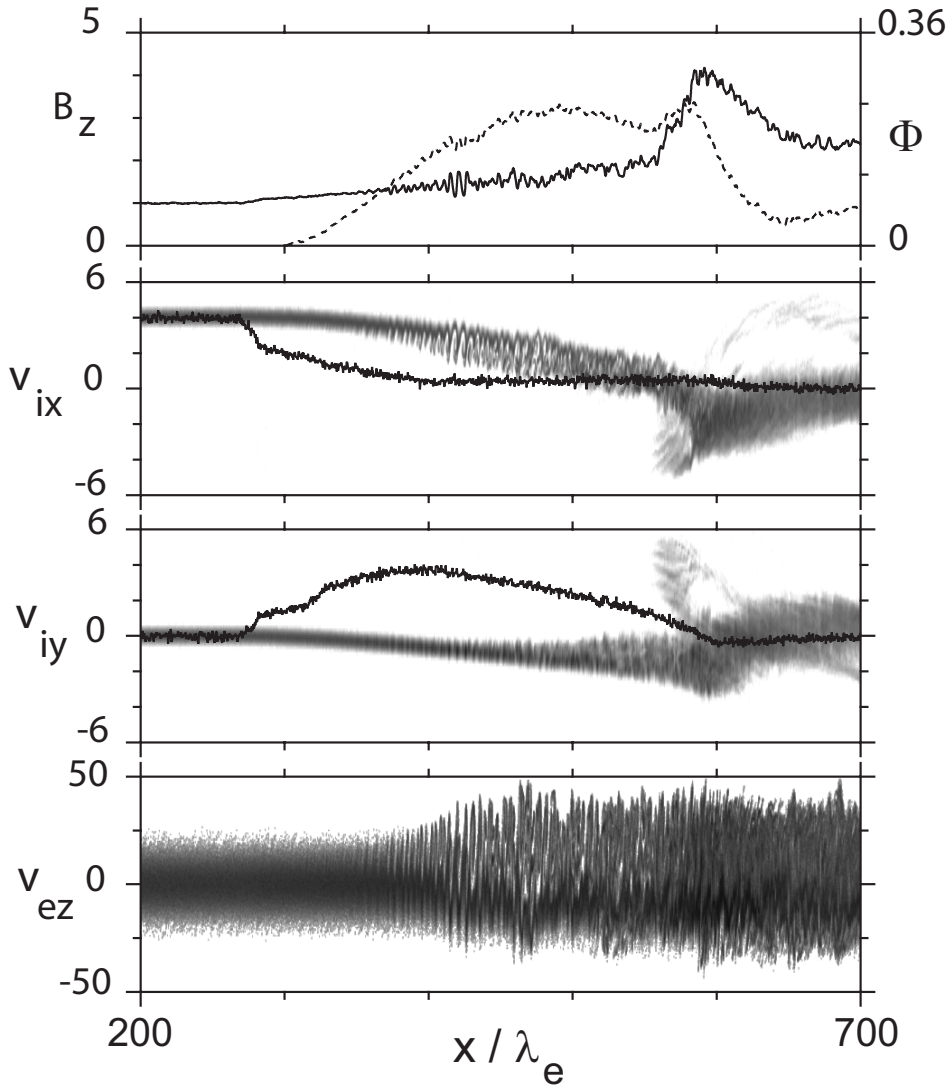

Figure 8. Results from run B ($\Theta_{Bn} = 87°$, 30% pickup ions) in the same format as Figure 1.

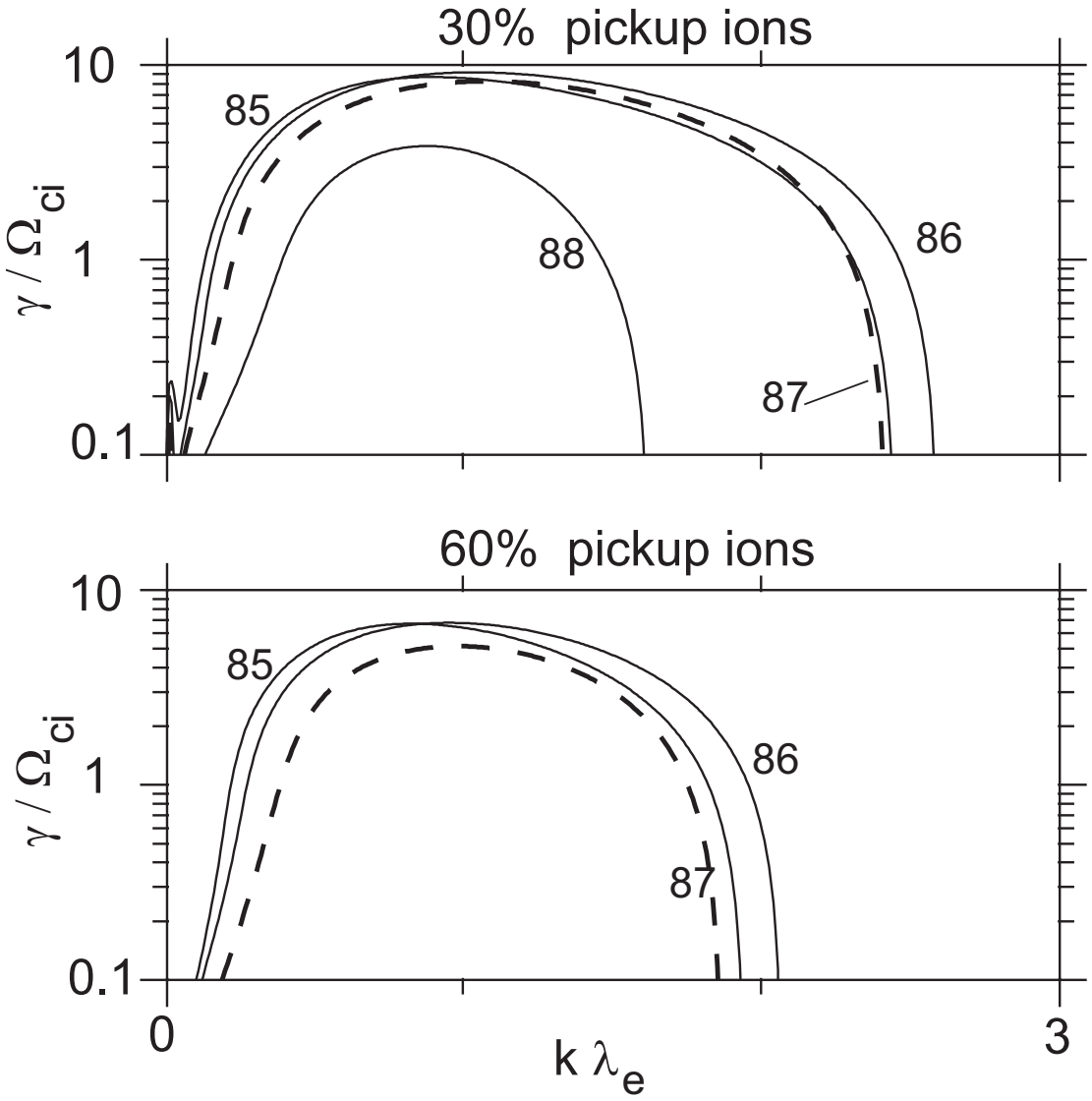

Figure 9. Growth rate γ of the modified two-stream instability versus wave vector k for different angles Θ_{Bn}. The upper panel shows the result for the 30% pickup ion case and the lower panel shows the result for the 60% pickup ion case, respectively.

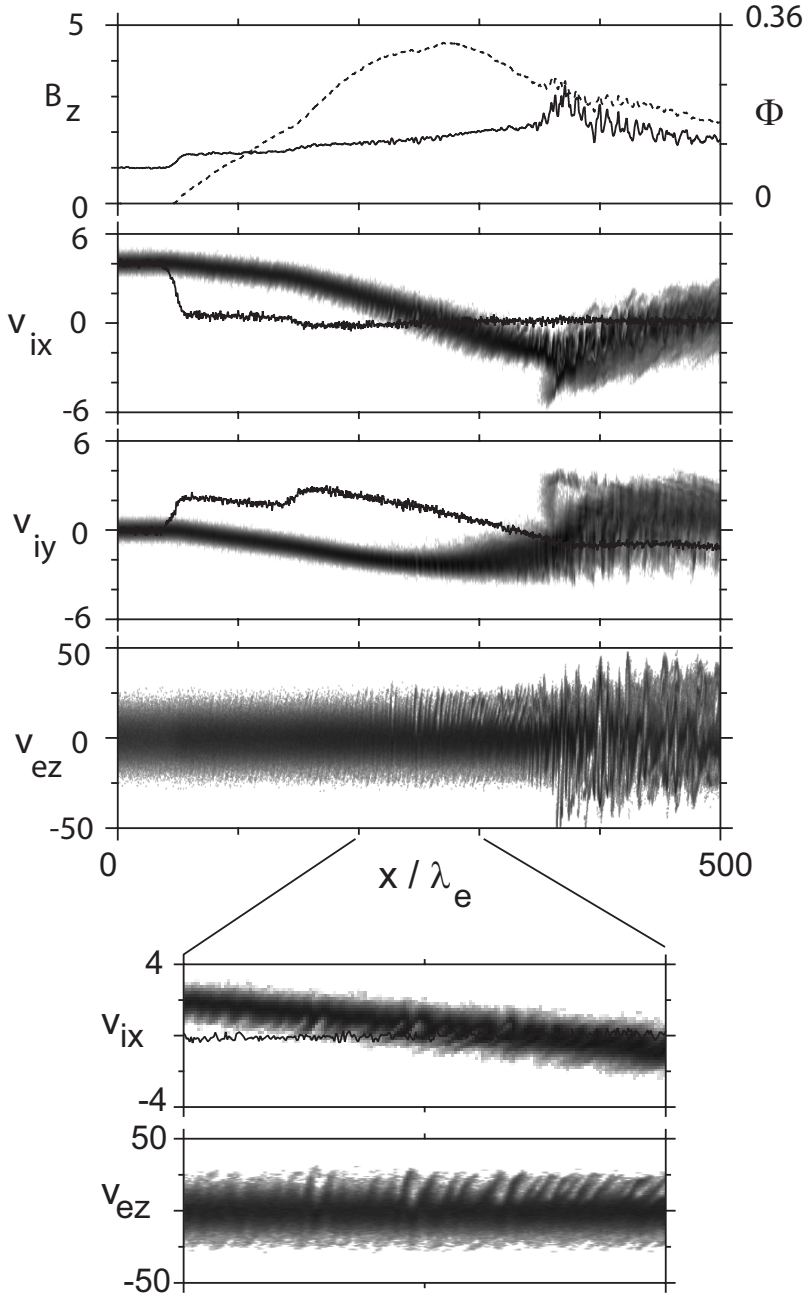

Figure 10. Upper part: Results from run C ($\Theta_{Bn} = 87°$, 60% pickup ions) in the same format as Figure 1. Lower part: Blow up of v_{ix} and v_{ez} over part of the foot ($200 \leq x \leq 300$).

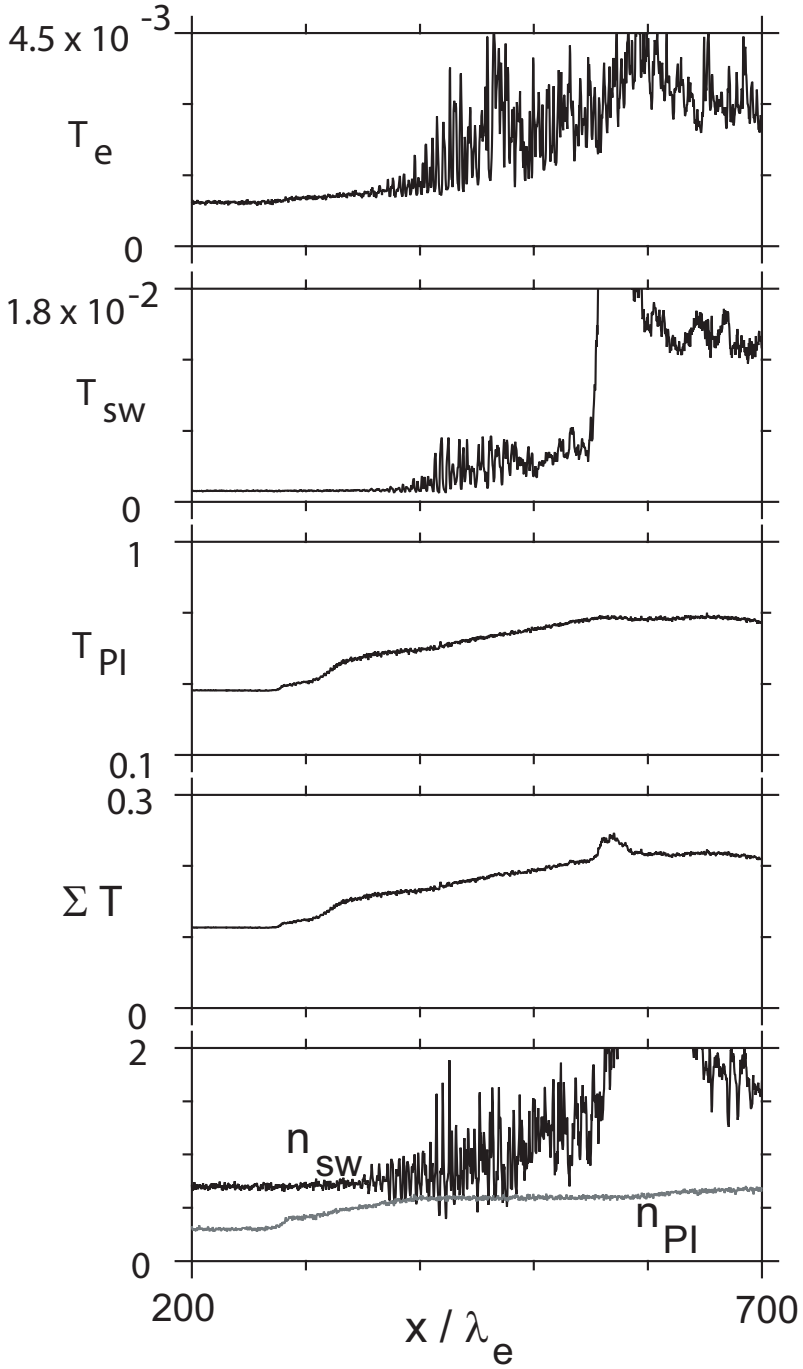

Figure 11. Results from run B ($\Theta_{Bn} = 87°$, 30% pickup ions). From top to bottom: electron temperature, solar wind ion temperature, pickup ion temperature, total temperature, solar wind ion and pickup ion densities.

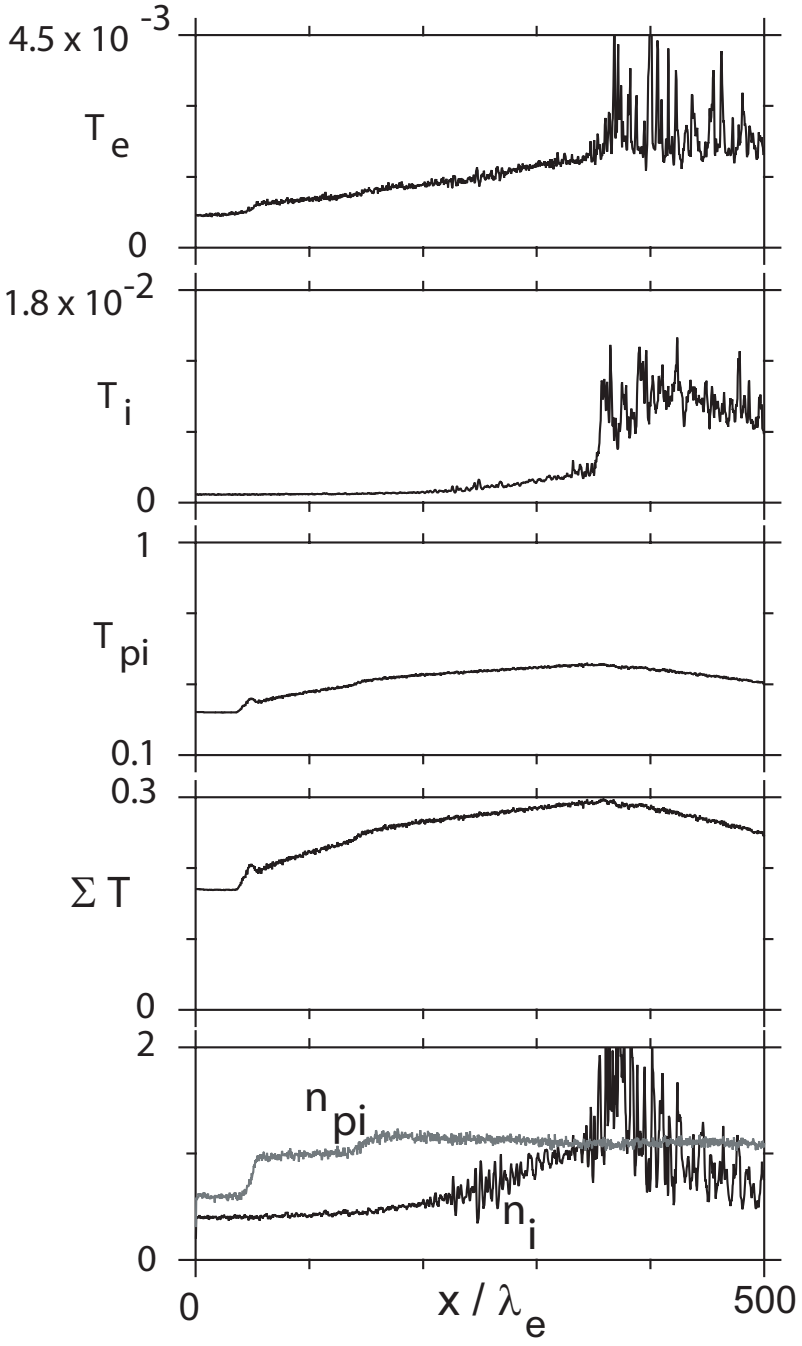

Figure 12. Same as Figure 11 for run C ($\Theta_{Bn} = 87°$, 60% pickup ions)

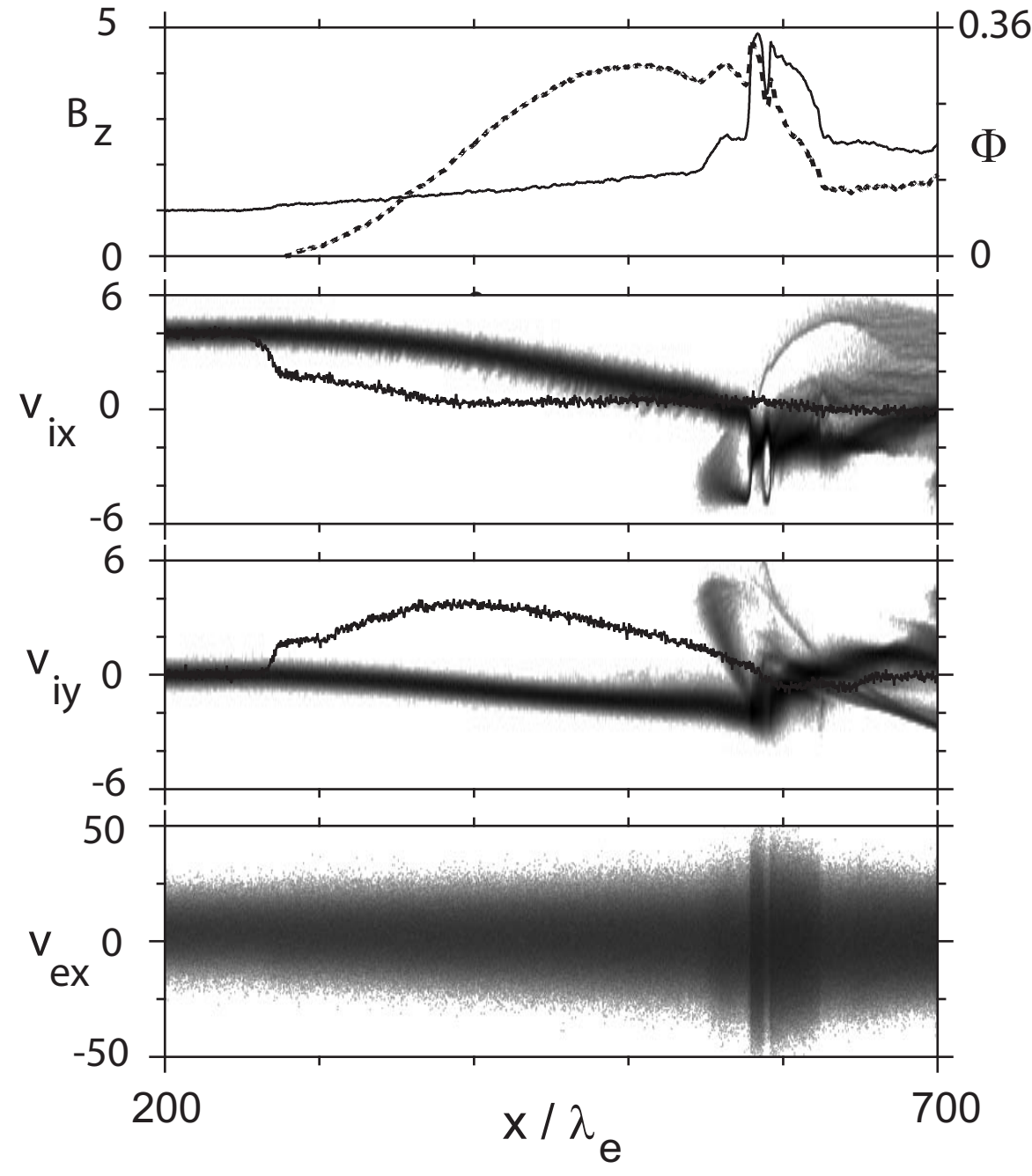
5
0
B_z
0.36
Φ
0
6
0
-6
v_{ix}
6
0
-6
v_{iy}
50
0
-50
v_{ex}
200
700
x / λ_e

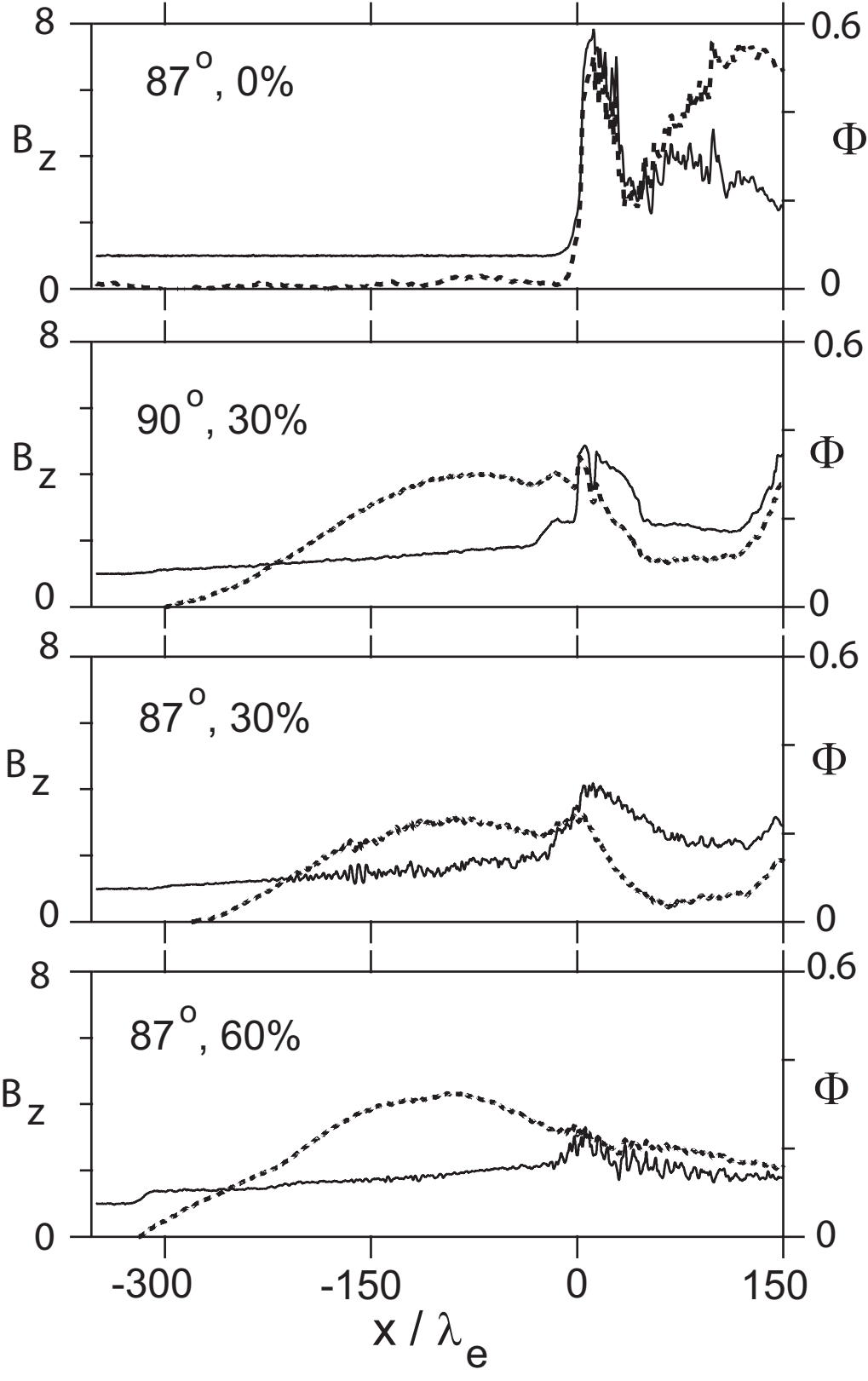
8
0.6
87°, 0%
B z
Φ
0
8
0.6
90°, 30%
B z
Φ
0
8
0.6
87°, 30%
B z
Φ
0
8
0.6
87°, 60%
B z
Φ
0
-300
-150
0
150
x / λ e

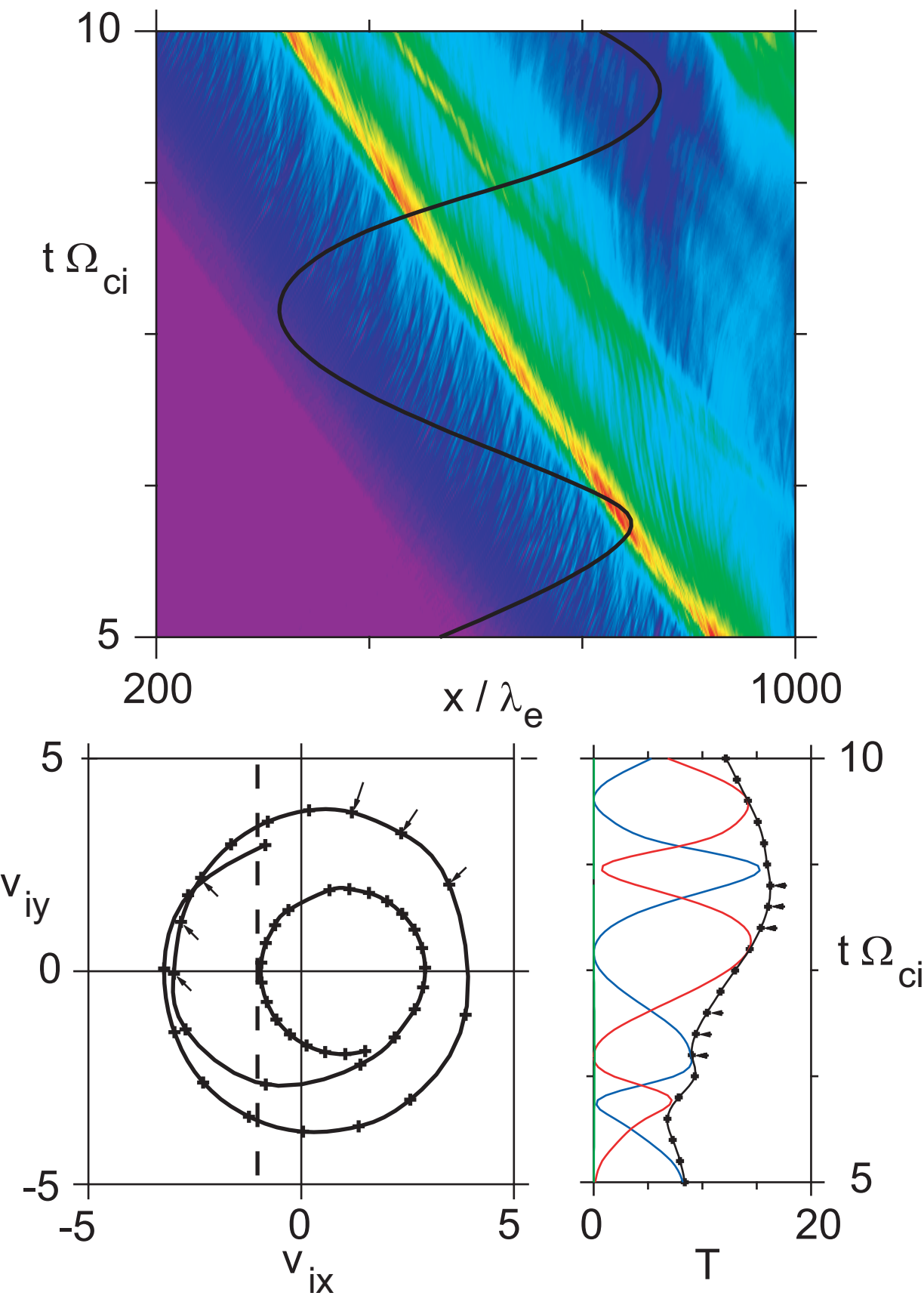
10
t Ω ci
5
200
x / λe
1000
5
viy
0
-5
-5
0
5
vix
10
t Ω ci
5
0
20
T

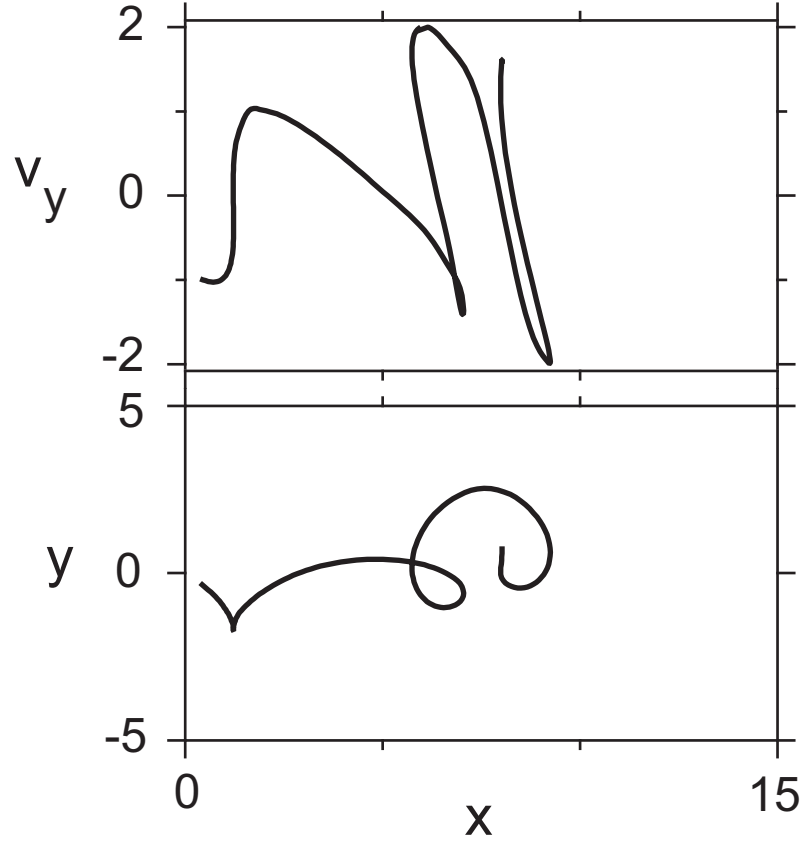
2
0
-2
v_y
5
0
-5
y
0
15
x

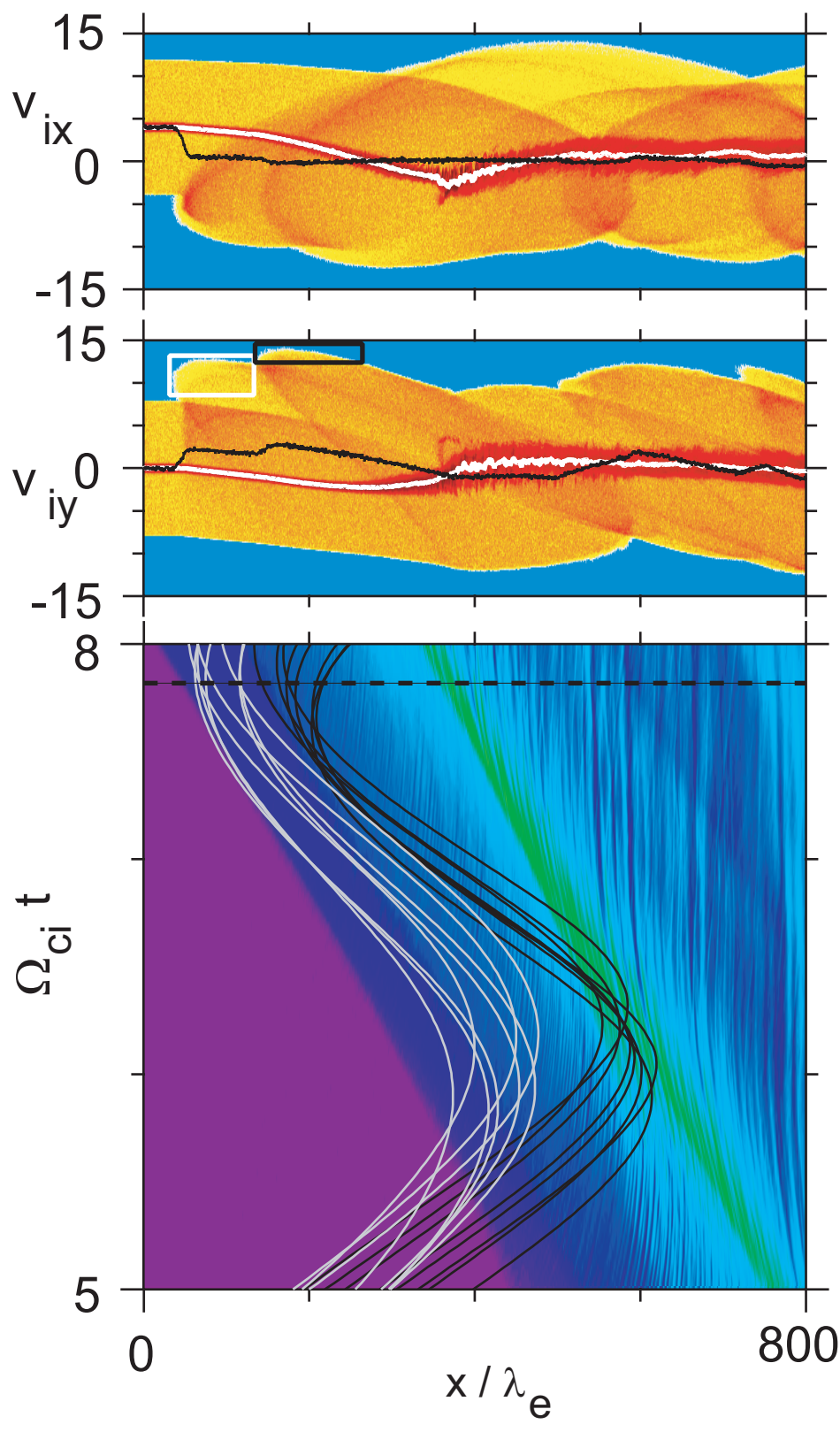
15
v ix
0
-15
15
v iy
0
-15
8
Ω ci t
5
0
800
x / λ e

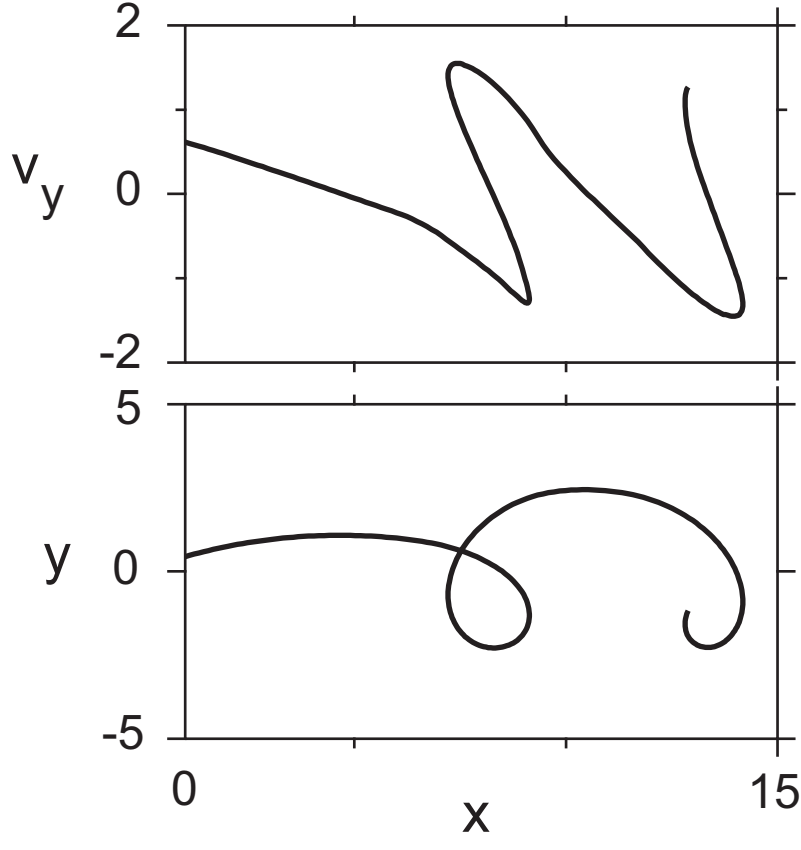
2
v_y
0
-2
5
y
0
-5
0
15
x

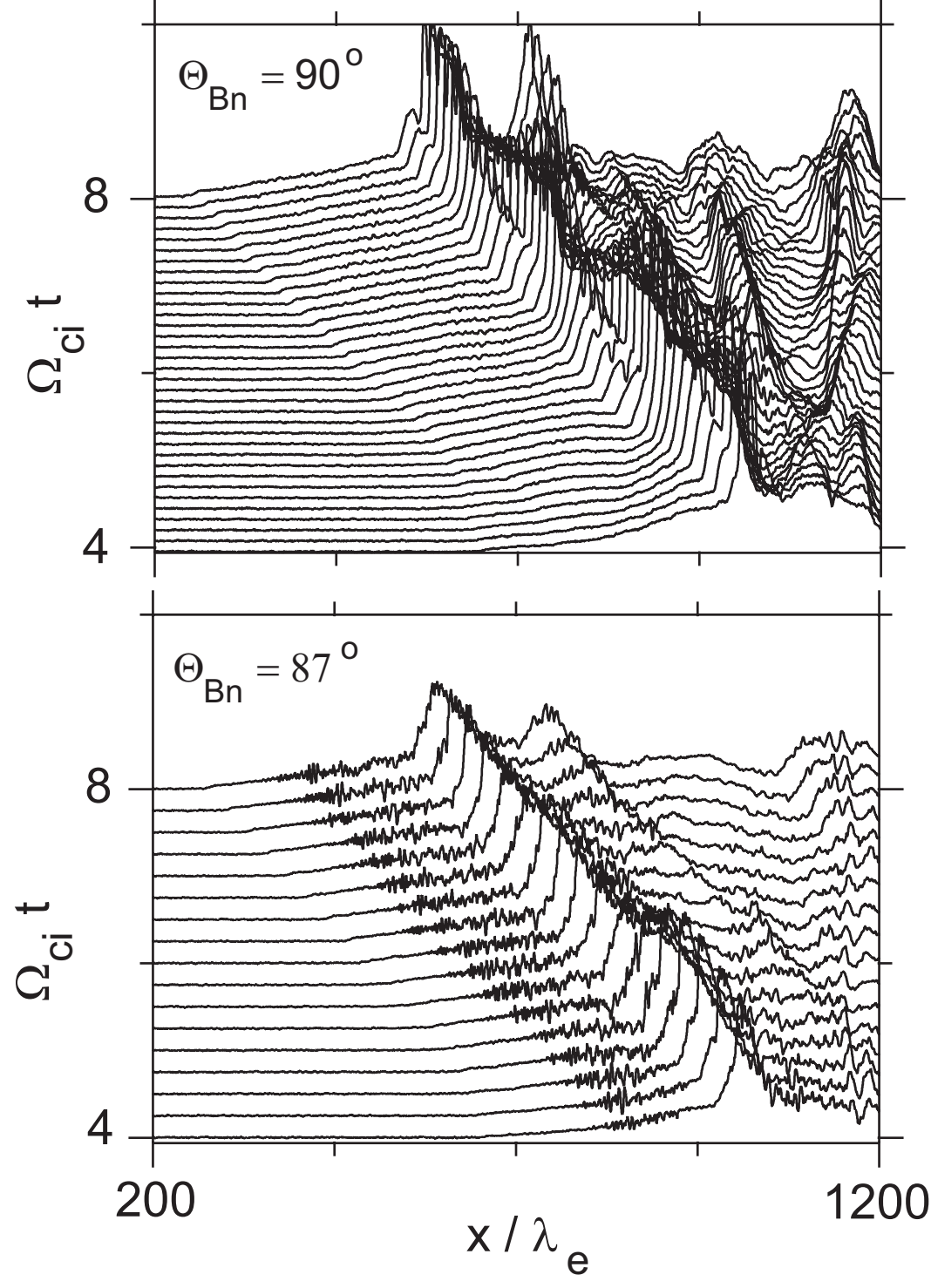
$\Theta_{Bn} = 90^o$
8
4
$\Omega_{ci}\, t$
$\Theta_{Bn} = 87^o$
8
4
$\Omega_{ci}\, t$
200
1200
x / λ_e

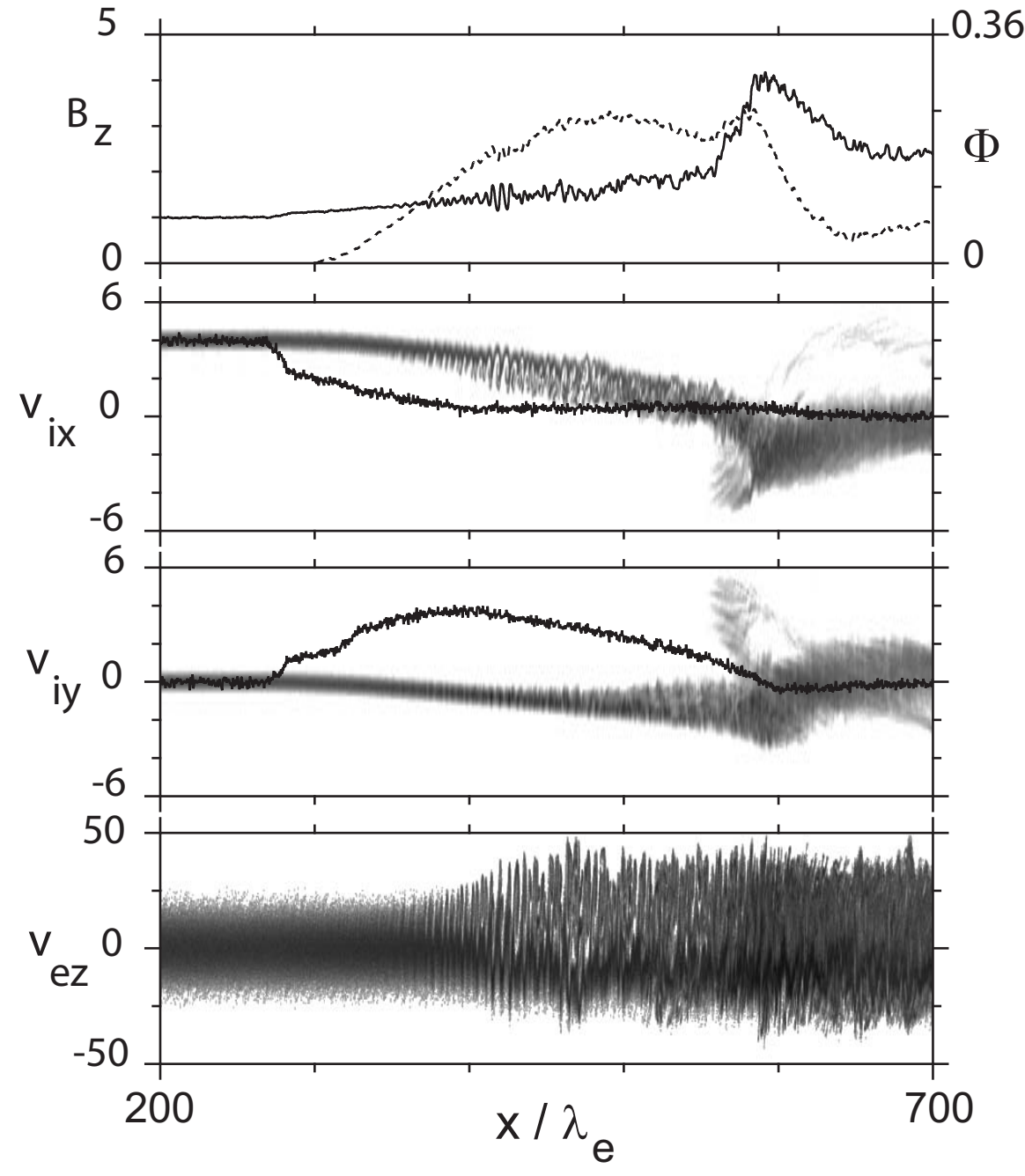
5
0.36
B_z
Φ
0
0
6
v_{ix}
0
-6
6
v_{iy}
0
-6
50
v_{ez}
0
-50
200
700
x / λ_e

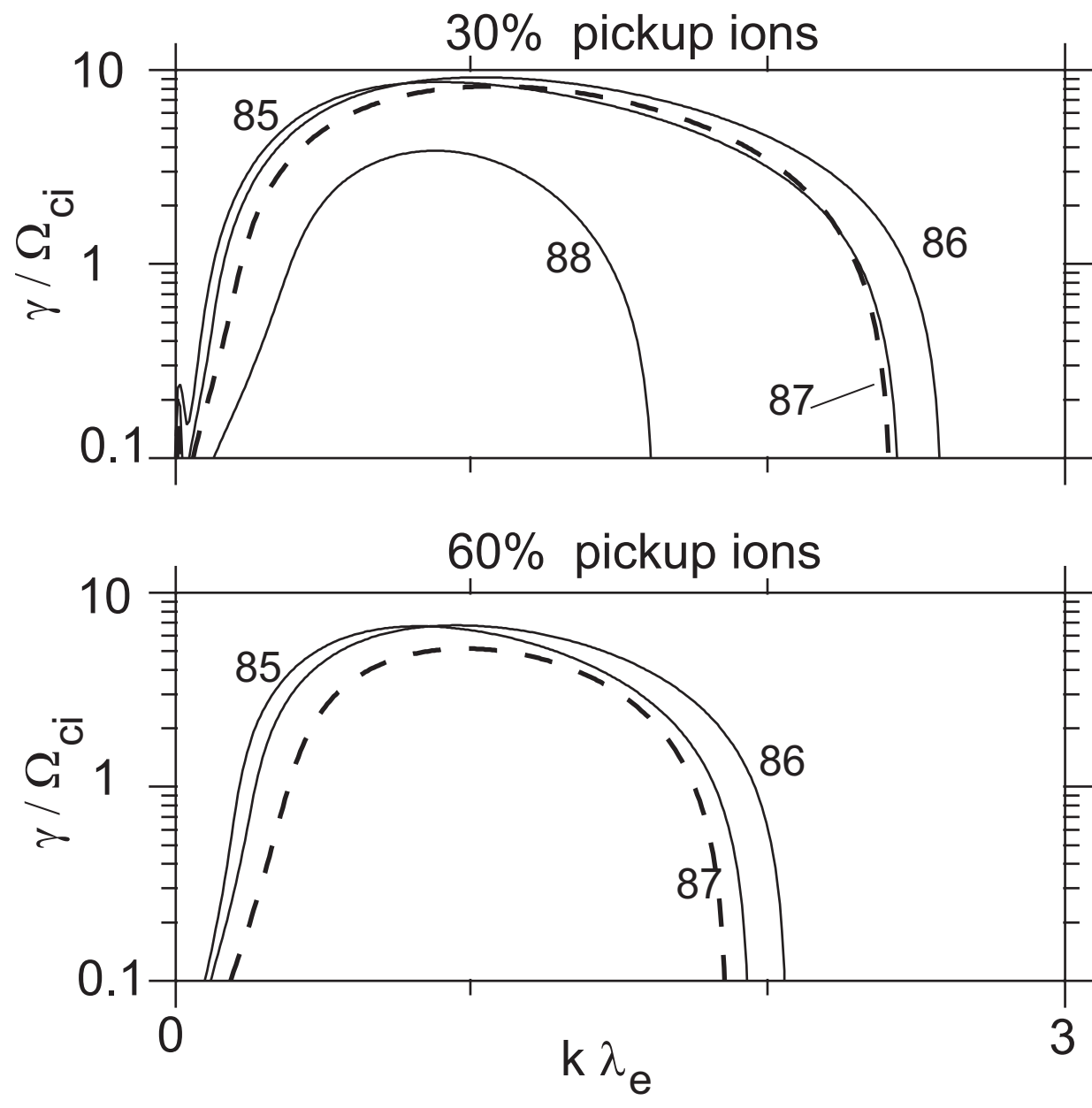
30% pickup ions
10
1
0.1
γ / Ω_ci
85
86
87
88
60% pickup ions
10
1
0.1
γ / Ω_ci
85
86
87
0
3
k λ_e

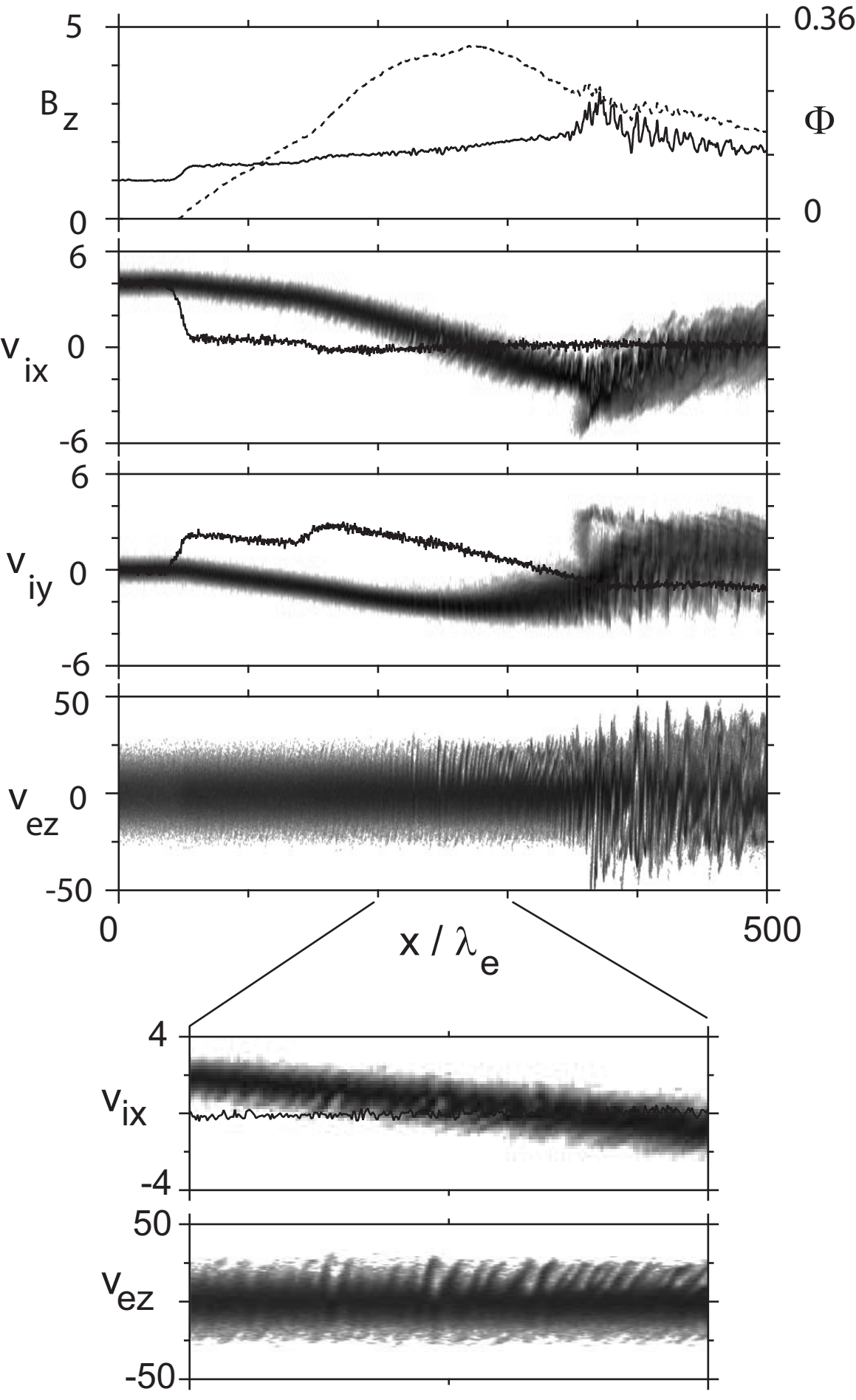
5
0
B_z
0.36
Φ
0
6
0
-6
v_{ix}
6
0
-6
v_{iy}
50
0
-50
v_{ez}
0
500
x / λ_e
4
-4
v_{ix}
50
-50
v_{ez}

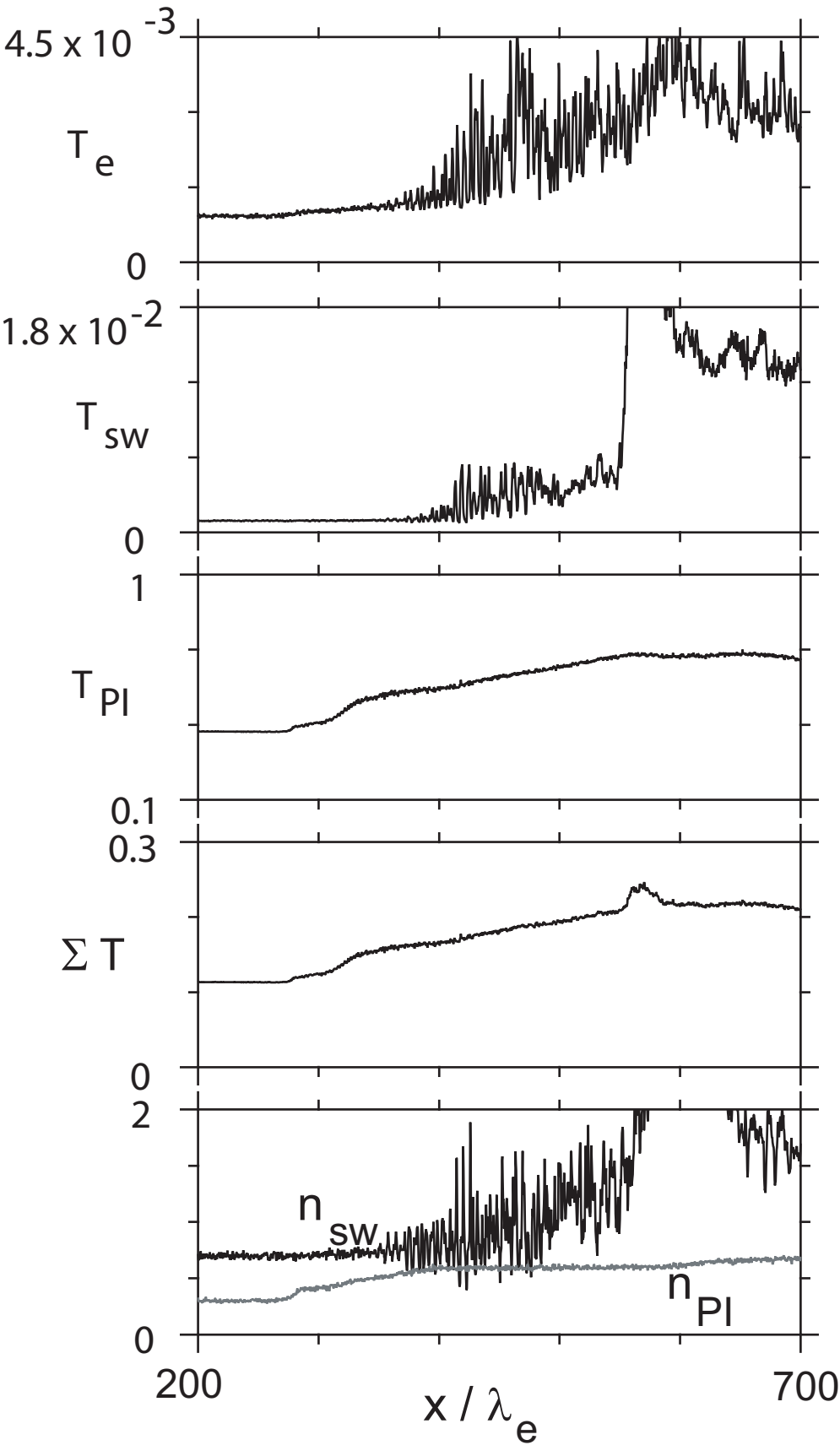
4.5 x 10 -3
T e
0
1.8 x 10 -2
T sw
0
1
T Pl
0.1
0.3
Σ T
0
2
n sw
n Pl
0
200
700
x / λ e

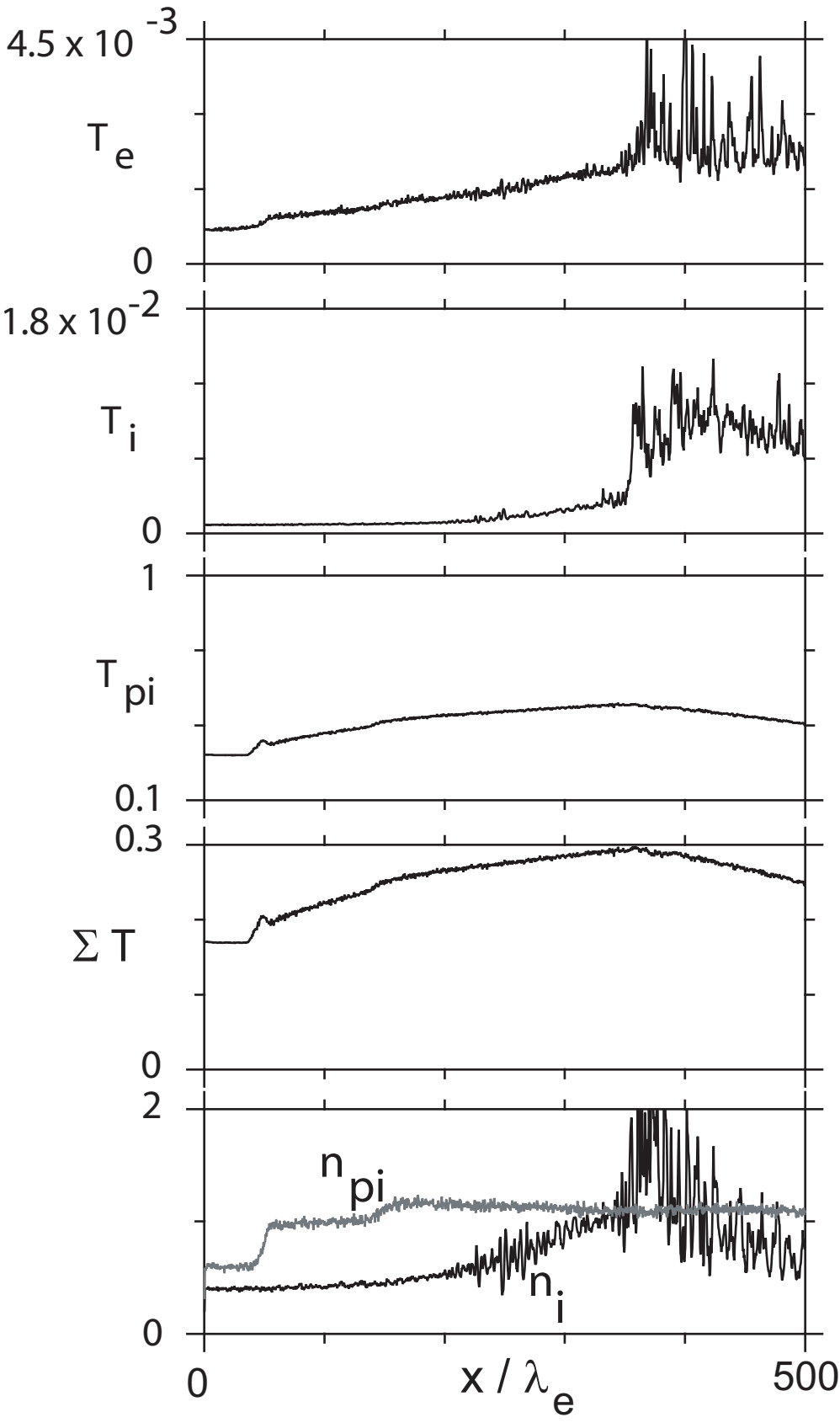
4.5 x 10 -3
T e
0
1.8 x 10-2
T i
0
1
T pi
0.1
0.3
Σ T
0
2
n pi
n i
0
0
x / λ e
500